New phagotrophic euglenoid species (new genus *Decastava*; *Scytomonas saepesedens*; *Entosiphon oblongum*), Hsp90 introns, and putative euglenoid Hsp90 pre-mRNA insertional editing

Thomas Cavalier-Smith[a,*], Ema E. Chao[a], Keith Vickerman[b,†]

[a]*Department of Zoology, University of Oxford, South Parks Road, Oxford OX1 3PS, UK*
[b]*Division of Environmental and Evolutionary Biology, University of Glasgow, Glasgow C12 8QQ, UK*

Abstract

We describe three new phagotrophic euglenoid species by light microscopy and 18S rDNA and Hsp90 sequencing: *Scytomonas saepesedens*; *Decastava edaphica*; *Entosiphon oblongum*. We studied *Scytomonas* and *Decastava* ultrastructure. *Scytomonas saepesedens* feeds when sessile with actively beating cilium, and has five pellicular strips with flush joints and *Calycimonas*-like microtubule-supported cytopharynx. *Decastava*, sister to *Keelungia* forming new clade Decastavida on 18S rDNA trees, has 10 broad strips with cusp-like joints, not bifurcate ridges like *Ploeotia* and *Serpenomonas* (phylogenetically and cytologically distinct genera), and *Serpenomonas*-like feeding apparatus (8–9 unreinforced microtubule pairs loop from dorsal jaw support to cytostome). Hsp90 and 18S rDNA trees group *Scytomonas* with *Petalomonas* and show *Entosiphon* as the earliest euglenoid branch. Basal euglenoids have rigid longitudinal strips; derived clade Spirocuta has spiral often slideable strips. *Decastava* Hsp90 genes have introns. *Decastava/Entosiphon* Hsp90 frameshifts imply insertional RNA editing. *Petalomonas* is too heterogeneous in pellicle structure for one genus; we retain *Scytomonas* (sometimes lumped with it) and segregate four former *Petalomonas* as new genus *Biundula* with pellicle cross section showing 2–8 smooth undulations and typified by *Biundula* (=*Petalomonas*) *sphagnophila* comb. n. Our taxon-rich site-heterogeneous rDNA trees confirm that *Heteronema* is excessively heterogeneous; therefore we establish new genus *Teloprocta* for *Heteronema scaphurum*.
© 2016 The Author(s). Published by Elsevier GmbH. This is an open access article under the CC BY license (http://creativecommons.org/licenses/by/4.0/).

Keywords: *Biundula*; Decastavida; Hsp90 phylogeny; Spirocuta; *Teloprocta*; 18S rRNA phylogeny

Introduction

Euglenozoa are genetically and morphologically the most distinctive protozoan phylum (Cavalier-Smith 1981). They are ancestrally aerobic, non-pseudopodial zooflagellates with a microtubule-rich pellicle, a unique complex feeding apparatus (FA), tubular extrusomes, parallel centrioles attached within a deep ciliary pocket by three distinctive microtubular roots to the pellicle and FA, and cilia ancestrally with unique dissimilar latticed paraxonemal rods (Cavalier-Smith 1981, 1995; Simpson 1997). Free-living Euglenozoa almost all have two centrioles and abound in virtually all freshwater, soil, and marine habitats; they can be phagotrophic, photosynthetic, osmotrophic, or depend on ectosymbiotic

---

bacteria (Yubuki et al. 2009, 2013). Symbiotic in animals are the parasitic, often secondarily uniciliate, Trypanosomatida (some causing serious human diseases, e.g. sleeping sickness, leishmaniasis), and the tadpole-gut-commensal euglenamorphids that multiplied their centrioles to 3–7 (Hegner 1923). Biciliate Euglenozoa also can parasitize animals (*Cryptobia*, *Trypanoplasma*) or plants (*Phytomonas*). Nuclear and mitochondrial genomes of all Euglenozoa have numerous unusual properties (Cavalier-Smith 1993a; Lukeš et al. 2009; Marande et al. 2005; Roy et al. 2007; von der Heyden et al. 2004). Some of these bizarre oddities, such as mitochondrial genome pan-editing and euglenozoan nuclear mRNA biogenesis by universal nuclear trans-splicing of mini-exons onto immensely long multigenic transcripts, are clearly highly derived not primitive eukaryotic features (Cavalier-Smith 1993a). In contrast, many unique molecular features, some more like those of archaebacteria than other eukaryotes or apparently primitive in various ways, suggest that Euglenozoa may be the most divergent of all protozoan and eukaryote phyla (Cavalier-Smith 2010) and of exceptional evolutionary interest (Cavalier-Smith 2013). This position of the root of the eukaryotic tree is also supported by some ribosomal multiprotein trees with prokaryote outgroups (Lasek-Nesselquist and Gogarten 2013) and by the uniqueness of 19 kinetoplastid kinetochore proteins (Akiyoshi and Gull 2013) – but questioned by similar mitochondrial multiprotein trees (Derelle et al. 2015).

Despite their key importance for understanding eukaryote early evolution, relationships among the four major ultrastructurally distinctive euglenozoan groups (Cavalier-Smith 1998) and therefore the nature of the ancestral euglenozoan remain unclear, as rDNA trees have been repeatedly contradictory. Phylogenetic trees for several proteins indicated that classes Kinetoplastea (trypanosomatids and their free-living bodonid and prokinetoplastid relatives) and Diplonemea are sister groups (Simpson et al. 2006; Simpson and Roger 2004), contradicting earlier classification into subphyla (Cavalier-Smith 1993b) and early 18S rDNA trees (von der Heyden et al. 2004). Unlike the purely heterotrophic kinetoplastids and diplonemids, euglenoids of all nutritional modes are characterized by a pellicle supported by longitudinal or spiral proteinaceous pellicular strips as well as microtubules (mts). Multiprotein trees based on 187–192 genes robustly confirm the Kinetoplastea/Diplonemea clade (Cavalier-Smith et al. 2014; Cavalier-Smith 2016). But whether this clade is sister to or evolutionarily derived from the cytologically more diverse euglenoids has not been established because neither basal euglenoids nor the enigmatic Postgaardea (=Symbiontida) have been subjected to large-scale sequencing, so are absent from gene-rich trees.

The status of the anaerobic class Postgaardea (Cavalier-Smith 1998) of heterotrophs densely clothed in episymbiotic bacteria was recently partially clarified by rDNA sequencing *Calkinsia* and a new genus *Bihospites*: Postgaardea form a clade so deep branching within Euglenozoa that its precise position is uncertain (Breglia et al. 2010; Yubuki et al. 2009). *Calkinsia*, classically thought a euglenoid (Lackey 1960; Leedale 1967, 2002), was transferred to Postgaardea by Cavalier-Smith (2003). This clade was needlessly renamed Symbiontida (Yubuki et al. 2009), but ultrastructural similarity of *Calkinsia*, *Bihospites*, and *Postgaardi* (Yubuki et al. 2013) supports all three belonging in Postgaardea. The discovery that *Bihospites* has relatively complex FA with two curved 'rods' of novel structure, led Yubuki et al. (2013) to suggest that postgaardeans evolved by substantial modifications of euglenoid pellicle and FA.

An 18S rDNA tree (Yubuki et al. 2009) weakly suggested that euglenoids may be paraphyletic and both postgaardeans and the diplonemid/kinetoplastid clade might be derived from them, but another (Chan et al. 2015) did not even show the diplonemid/kinetoplastid clade, whose reality was firmly established by 192-protein trees (Cavalier-Smith et al. 2014). 18S rDNA trees of Yamaguchi et al. (2012), Lax and Simpson (2013), and Chan et al. (2015) also placed postgaardiids (but not kinetoplastids) weakly within euglenoids, and Lee and Simpson (2014a,b) controversially treat them as euglenoids, though trees of Chan et al. (2013) equally weakly put them between diplonemids and kinetoplastids. Those of Chan et al. (2013) and Lax and Simpson (2013) placed Kinetoplastea as sister to all other Euglenozoa as in early distance trees (von der Heyden et al. 2004), which 187-protein trees including both prokinetoplastids and metakinetoplastids decisively refute (Cavalier-Smith et al. 2016). Poor resolution of the deep branching order of Euglenozoa on 18S rDNA trees suggests rapid early radiation, but may be exacerbated by insufficient taxon sampling of early phagotrophic lineages and unequal rates of evolution with extra-long branches for *Entosiphon* and rhabdomonads.

To reduce or circumvent these problems we sequenced 18S rRNA and Hsp90 genes from three previously undescribed phagotrophic euglenoids isolated and studied ultrastructurally some years ago by Vickerman (unpublished) so as to produce trees for Euglenozoa with broader taxon sampling. We describe all three as new species and show novel ultrastructural features for two. One is a *Scytomonas* from manure, unique among euglenoids in feeding whilst attached by its cell posterior to surfaces with actively beating single cilium that draws bacteria to its mouth. Most phagotrophic euglenoids feed whilst actively gliding and generally have two cilia. To test the widespread assumption that Euglenozoa were ancestrally biciliate and establish the ancestral phenotype for euglenoids it is important to know whether *Scytomonas*, the only genus with a single cilium and centriole (Mignot 1961), is primitively uniciliate or evolved from biciliate ancestors by losing the second centriole; this will help reconstructing the last common ancestor of all eukaryotes from which Euglenozoa and excavates probably diverged (Cavalier-Smith 2010; Cavalier-Smith 2014b). *Scytomonas* proves to be phylogenetically sister to *Petalomonas* as here revised, showing that its single cilium and centriole is a secondary reduction. Thus the last common ancestor of all Euglenozoa had two centrioles – also true for eukaryotes

as a whole, whether the eukaryote tree's root is really between Euglenozoa and Excavata (Cavalier-Smith 2010, 2013; Lasek-Nesselquist and Gogarten 2013), as we argue, or between discicristates (Euglenozoa plus Percolozoa) and other eukaryotes as another ribosomal protein multigene tree suggests (Raymann et al. 2015), or between podiates and other eukaryotes as a different multigene set suggests (Derelle et al. 2015). Our second new euglenoid is a very deep branching relative of recently described *Keelungia pulex* (Chan et al. 2013), differing sufficiently to merit a new genus *Decastava*; we establish new order Decastavida for them. We discuss the evolutionary significance of the novel ultrastructure of *Decastava* and *Scytomonas saepesedens*.

The third new euglenoid is *Entosiphon oblongum*, closely related to *Entosiphon sulcatum*, but differing in shape and rDNA and Hsp90 sequences. Its characterization clarifies past conflicts in the shape depicted for *E. sulcatum* (Huber-Pestalozzi 1955; Lemmermann 1913; Ritter von Stein 1878) and suggests that two separate species were often lumped under one name. Previously *Entosiphon* rDNA exhibited serious long-branch problems that yielded highly conflicting trees preventing its accurate phylogenetic assignment (von der Heyden et al. 2004; Lax and Simpson 2013). Our Hsp90 trees are not seriously affected by long-branch artefacts, suggesting that this protein may be particularly useful for euglenozoan phylogeny and that *Entosiphon* is probably sister to all other euglenoids. Our discovery of frameshifts in Hsp90 genes of both and *Entosiphon* and *Decastava* give the first evidence for putative nuclear insertional RNA editing in Euglenozoa.

Material and Methods

Cultures. (a) *Scytomonas*. A sample from an exposed heap of horse manure, taken about eight weeks after stacking, was steeped in Cerophyll-Prescott medium (dried grass infusion; Page 1988) and after one week surface film material containing an abundant *Vahlkampfia* species was transferred to cerophyll agar plates. *Scytomonas* appeared when plates were flooded with fresh Cerophyll-Prescott infusion and was separated from accompanying amoebae by dilution. Further cultivation was with accompanying mixed bacterial flora in 3–4 mm depths of Cerophyll-Prescott medium in flat 50 ml Falcon flasks, with subculture at fortnightly intervals. (b) *Entosiphon oblongum* and *Decastava edaphica* were isolated from Scottish soil (Falkland Palace Gardens and Sourhope, respectively). For light microscope observations and DNA extraction by standard methods (Howe et al. 2011a) all three euglenoids were grown in Volvic^{TM} mineral water in Petri dishes with an added boiled wheat grain to feed endogenous bacteria as food for the euglenoids.

Microscopy. Cells were observed by phase contrast and differential interference microscopy (DIC) and photographed using a X60 W dipping water immersion immersion objective on a Nikon Eclipse 80i microscope (Nikon, Tokyo, Japan) and a Sony HDV 1080i Handycam (Sony, Tokyo, Japan). They were prepared for scanning and transmission microscopy by fixation in 2% glutaraldehyde and subsequent processing as described by De Jonkheere et al. (1984).

PCR and sequencing. 18S rDNA was amplified by standard eukaryote-wide primers and sequenced directly (Howe et al. 2011a). For Hsp90 nested amplification (Stechmann and Cavalier-Smith 2003) using modified primers (Yabuki et al. 2012) was followed by agarose electrophoretic gel purification of bands and cloning into the pSC-A vector using the Strata-Clone PCR Cloning kit (Stratagene) before ABI automated sequencing.

Phylogeny. We used macgde v. 2.4 (http://macgde.bio.cmich.edu/) for manual alignment and site selection of well aligned regions by eye for analysis. Phylogenetic analysis was by RAxMLHPC-PTHREADS-SSE3 v. 7.3.0 (Stamatakis 2006) using the GAMMA model with four rate categories and fast bootstraps (4 processors) and by the evolutionarily more realistic and often more accurate site-heterogeneous CAT-GTR-GAMMA (4 rates) model of PhyloBayes v. 3.3 (Lartillot and Philippe 2004) with two chains for thousands of generations after log likelihood values plateaued, early pre-plateau trees being removed as burnin before summation of all other trees (for brevity called CAT only in the text). RAxML used the GTR substitution model for rDNA trees and the LGF substitution model for Hsp90. For Hsp90 all Bayesian trees converged with maxdiff <0.3, mostly 0.1 or less. For 18S rDNA we manually aligned 18S rDNAs of 217 Euglenozoa plus 481 outgroup taxa representing all major eukaryote groups and selected by eye 1577 or 1541 reasonably well aligned nucleotide positions for preliminary phylogenetic analysis (>50% more than in some euglenozoan studies), depending on whether the highly divergent Percolozoa were excluded or included. To investigate the effect of taxon sampling and site selection we ran 16 rDNA trees with different taxon and sequence samples and algorithms. The methods, rationale, and results for these numerous 18S rDNA trees are described in detail in a separate paper on euglenozoan phylogeny and higher classification (Cavalier-Smith 2016); some of these Bayesian trees converged well and some did not. Simply to show the positions of our new species, a composite figure combining results from the 282-taxon tree (excluding *Entosiphon*) and the 287-taxon tree including *Entosiphon* is shown here as supplementary Fig. S1. Trees were prepared for publication using FigTree v. 1.2.2 (http://tree.bio.ed.ac.uk/software/figtree/) and Eazydraw.

Results

Morphology of *Scytomonas saepesedens*

The flagellate is 8–14 μm long and 5–10 μm maximum width with a single cilium ~20 μm long (Fig. 1A–E). It has three modes of life. It glides along the substratum in characteristic *Petalomonas*-like fashion with the single cilium held
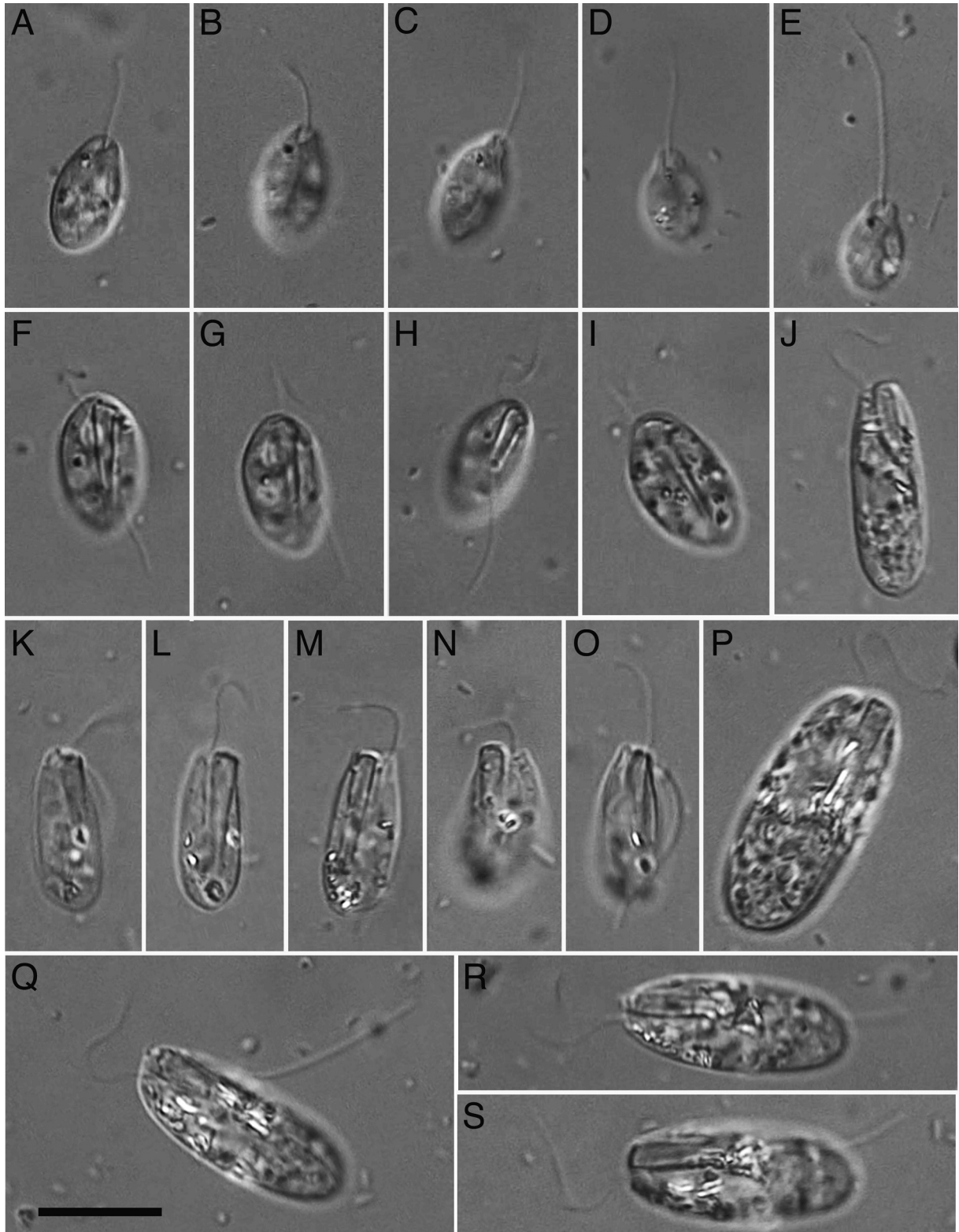
Fig. 1. Differential interference contrast micrographs of actively gliding flagellates. **A–E** *Scytomonas saepesedens*. **B, C** Different focal levels of same cell. **F–I** *Decastava edaphica.* **F, G** same cell; **H, I** another cell. **J–S** *Entosiphon oblongum*. **KLM** same cell showing retracted (K) or extended (L) siphon; N separate cell with extended siphon; **O** separate cell with all three supporting rods in focus. **P** unusually large cell showing a pellicular striation. **QRS** a relatively larger cell than K–M, showing cell showing rod extension (R; three rods visible) and retraction (S). Scale bar 10 μm.
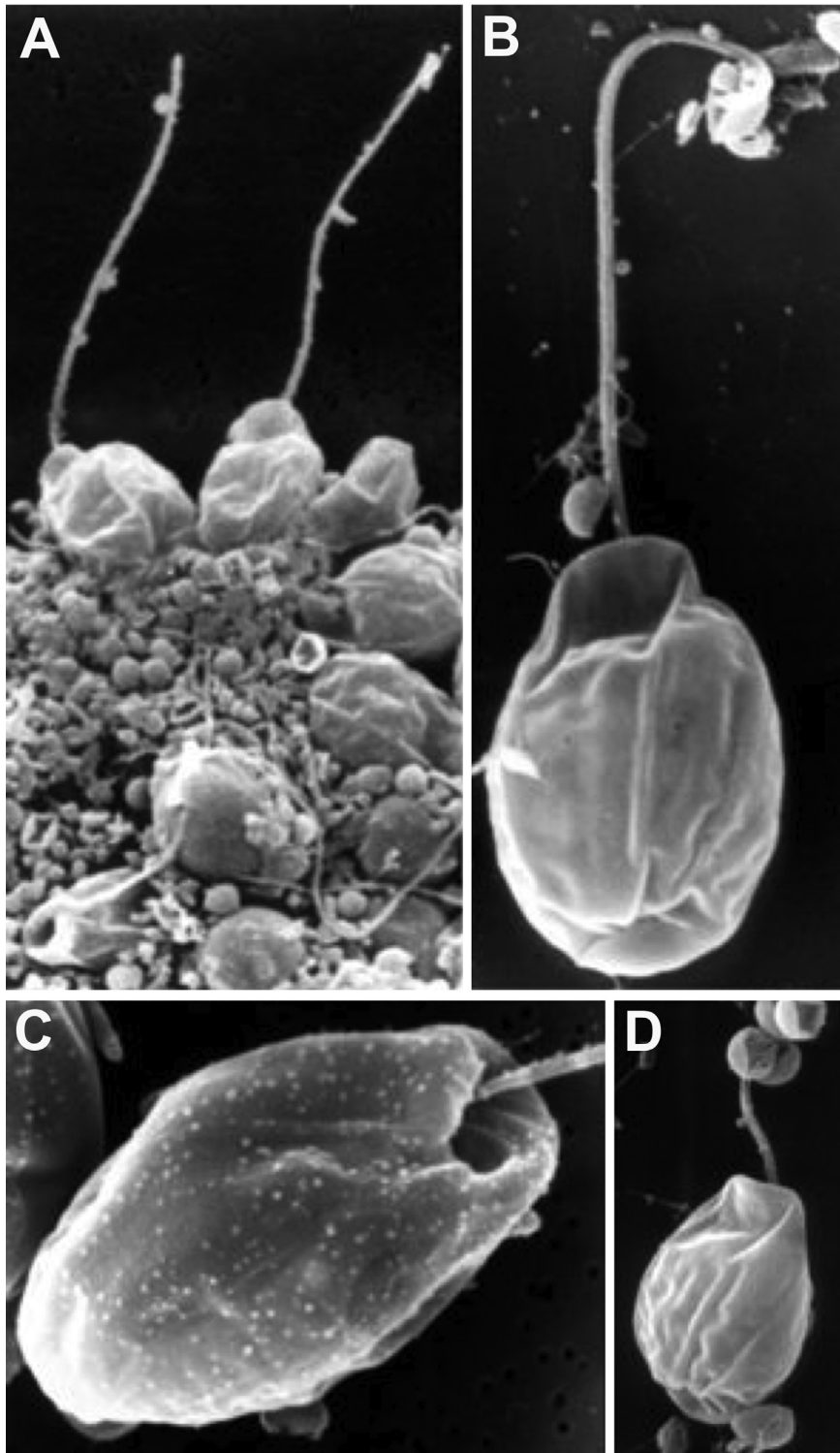
Fig. 2. Scanning electron micrographs of *Scytomonas saepesedens*. **A**. Cells with projecting apical cilium basally attached to a bacterial film. **B.** Cell with straight distally bent single cilium with associated rod-shaped bacteria and flattened shovel-like anterior end viewed dorsally. **C.** Ventral view of cell showing wide reservoir mouth with a single long emerging cilium and no second shorter one. **D.** Dorsal view of cell with coccoid bacteria sticking to the cilium.

out in front, only its terminal quarter beating. Its anterior end forms a pronounced collar, ventrally flattened, seemingly as a shovel-like scraper of bacteria from the substratum. Alternatively it attaches to the substratum or to bacterial debris by the posterior end whilst the cilium beats continuously and vigorously along its length, drawing bacteria towards the anterior mouth region. Stages in binary fission are observed in this sedentary form. A third phase is non-motile, more

phase-dense than the other two, has fewer refractile inclusions and no cilium; such forms become more abundant as the culture ages. On subculture these resting forms readily give rise to ciliated individuals.

A feeding cell can ingest quite large bacterial prey (e.g. *Selenomonas*) up to half its own size, yet has a rigid shape – unlike most macrophagous euglenoids having deformable pellicles. The body is typically pyriform (Fig. 1C–E) and lacks the noticeable flattening of *Petalomonas* spp. Scanning (SEM) and transmission electron microscopy show that the pellicle has five broad strips lacking grooves/troughs found in most euglenoids other than *Petalomonas* (Figs. 2–3). There are pleat-like thickenings of the pellicle strip joints similar to those of *Petalomonas cantuscygni* (Leander et al. 2001), but unlike that species the surface lacks projecting ridges, being most similar in SEM to the biciliate *Petalomonas mediocanellata* that was incorrectly assumed to lack strips (Leander et al. 2001). Strips are reinforced by underlying mts. Around the cilium the anterior end of the cell forms a pronounced collar (Fig. 2), more extended anteriorly on the ventral flattened side during gliding (Fig. 1A–E). Bacteria released from the substratum during gliding are trapped by the cilium membrane for transport to the cytostome for ingestion.

Only a single cilium can be seen in the trophic non-dividing flagellate; no second centriole (=basal body) was seen. From transmission micrographs it arises from the base of a deep ciliary pocket extending as much as half way down the body. No thick paraxonemal rod running alongside the axoneme of nine mt doublets was seen; but vestiges of such a structure are present (Fig. 4A) implying a very slender paraxonemal rod. On the opposite side to the putative rod vestige are densities suggestive of the dense sheets in similar positions in *Euglena* (Melkonian et al. 1982). The cilium transition zone is long and contains much dense material (Figs 3A, 4B). The single contractile vacuole empties into the ciliary pocket close to its base. The membrane lining the pocket is reinforced by mts (Fig. 4), but we did not serial section to determine their exact arrangement: apically (Fig. 4A) ten linked microtubules may be the dorsal row continuous with the five joint-associated pairs of dense pellicular microtubules; three nearby mts may be the dorsal centriolar root (DR). Near the junction of the cytostome and ciliary pocket are about five reinforced mts (MTR) at the ciliary pocket membrane and an adjacent mt pair that may be parallel mt loop (PML) mts that support a ridge separating the ciliary and cytostomal subregions of the reservoir (Fig. 4B). Ventrally to this ridge, the ciliary pocket is elongated by an extension with nearby fibrillar densities (Figs 3, 4B) and a dense arc strengthening the membrane near the cytostome (Figs 3B, 4B) on the opposite side from the putative MTRs. A prominent Golgi apparatus (dictyosome) composed of ∼15 cisternae is beside the ciliary pocket (Fig. 5A).

Arising from the ciliary pocket, just inside its opening on the cells left, the cytostome leads into a cytopharynx curving to the cell's right (seen from above during gliding), and reminiscent of that of kinetoplastids in its simplicity (Figs 5B, 6).

It consists of a membrane-bound channel supported by at least four reinforced supporting mts (Figs 5B, 6) and an arc of membrane thickening material with periodic dense structure (Fig. 5B) on opposite sides of the cytopharynx, as in the biciliate petalomonad *Calycimonas* (Triemer and Farmer 1991a,b). Two curved microfibrillar arcs are associated with the cytostome; the less obvious one nested within the more robust arc subtends a mixture of dense fibrillar material and microtubules (Figs 3A, 4B), which we suspect may be MTR and PML looped over from the ciliary pocket (see discussion). We suspect that the outer microfibrillar arc (Figs 3A, 4B) supports the collar. Elaborate mt-associated FA rods found in non-petalomonad phagotrophic euglenoids are absent. Food vacuoles containing bacterial remains abound in the cytoplasm. A hint of the long ciliary pocket/cytopharynx complex is sometimes evident on differential interference contrast (DIC) micrographs (Fig. 1C).

The interphase nucleus has typical euglenoid structure with chromatin masses (chromosomes) attached to the inner nuclear membrane and a large central nucleolus (Fig. 3A). A not-so-common feature is the presence of prominent bacterial symbionts in the cavity of the nuclear envelope and associated rough endoplasmic reticulum; one also sees bacteria within cytoplasmic vesicles (Fig. 6) possibly indirectly connected to the nuclear envelope lumen. Among the most obvious cytoplasmic inclusions are branches of the mitochondrial network with discoid cristae (Figs. 4–6). Hyperabundant "secretory vesicles" (e.g. Figs 3, 4A) are probably of Golgi origin and their external secretion might play a part in establishing anchorage on the substratum. Less easily identified membrane-bound bodies with electron-dense linings and a clear interior may be paramylon bodies or acidocalcisomes.

Morphology of *Decastava edaphica*

Decastava edaphica resembles some *Ploeotia* species in the light microscope in its ellipsoidal shape, but unlike in the type *P. vitrea* (Dujardin 1841) longitudinal striations are not obvious (Fig. 1F–I). Its anterior asymmetrically undulating (dorsal) cilium is less than one body length and posterior straight gliding (ventral) cilium projects from the rounded posterior by about a third of the body length in living cells, but less in the SEM of Fig. 7B. Cilia emerge from a nearly transversely oriented cleft-like reservoir that opens on the cell's right (seen from the dorsal side), the posterior cilium curving sharply backwards obliquely across the cell's ventral surface. Both cilia have typical euglenoid ultrastructure with a thick laminated posterior paraxonemal rod and more slender anterior one with a tubular lattice (Fig. 8). Its ventral non-protrusible feeding apparatus has two dense hollow rods, further apart at the front where they are joined by dense connectors, converging towards the cell posterior; the left rod begins more anteriorly and the right one extends further posteriorly (Fig. 1F–I). Though we did not obtain EM sections though the cytostome, from through-focal DIC microscopy
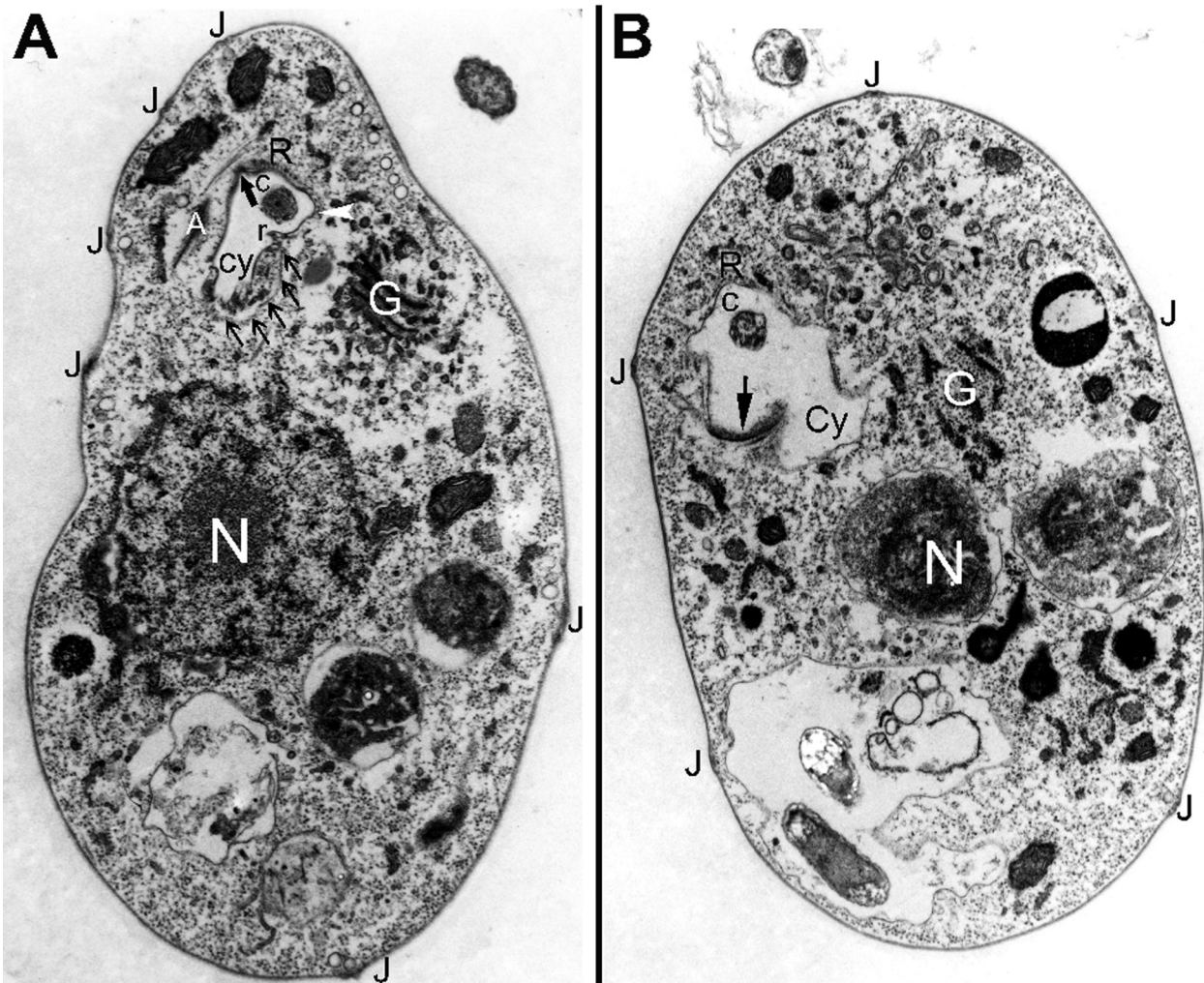
Fig. 3. Transmission electron micrographs of *Scytomonas saepesedens* showing a single cilium within the reservoir. In both cells the joints (J) between very broad pellicular strips are about twice as thick as the strips themselves but project only slightly as barely detectable ridges. **A.** Oblique section of cell with six strips (possibly partly duplicated) crossing the dense ciliary transition zone. Golgi (G) located beside the reservoir, and digestive vacuoles behind the heterochromatin-rich nucleus. The reservoir is differentiated into a ciliary pocket (c) and cytostomal region (Cy) delimited by a groove (thick arrow) with membrane-associated dense material and a ridge (r). A = part of putative anterior dense fibrillar collar support. R= dorsal mt row. White arrowhead marks dorsal centriolar root. N = nucleus. Thin arrows indicate the inner cytostome-associated microfibrillar arc that surrounds patches of dense fibrillar material. **B.** Transverse section showing five strips. The cytopharynx (Cy) is becoming separated from the ciliary pocket (c); arrow indicates the dense membrane-associated microfibrillar arc. Rod bacterium within digestive vacuole.

we suspect that there are two connectors, a straighter supporting its ventral lip (Fig. 1F) and a curved one on its dorsal side (Fig. 1G–J), which could make a nearly continuous dense ring around the mouth.

Electron microscopy shows that FA rods are hollow and composed of an extremely dense homogeneous matrix surrounding a lighter lumen; each has two dense lateral flanges (Fig. 8), dissimilar in cross section and orientation. The inner rod alongside the ciliary cleft has a very long inner flange that at least at its anterior extends far into the cell interior, nearly reaching the opposite (dorsal) side and probably supporting that entire flank of the cleft. Its opposite flange projects much less and is thinner, sharply tapered, and ends at a slight bulge in the pellicular strip at the mouth of the cleft; this strip is the

longest central ventral strip, tapers least anteriorly, and has a short anterior notch at the point of posterior ciliary inflection, which extends backwards just over a fifth of its length (Fig. 7B). The right (outer) rod is on the opposite side of the cytopharynx and its flanges are oriented transversely to the ventral surface of the cell. Its outer flange, associated with the extreme left edge of the next (right) ventral strip, is thinner and more tapered, but longer than in the inner rod; its inner flange is shorter and thicker, somewhat curved with a cusp like projection. At least six dense, relatively straight vanes are associated with the cytopharynx, four arranged as two parallel pairs (Fig. 8); one is markedly broader than the others but we did not determine their precise number or arrangement. The cemented feeding comb present on the other side of the
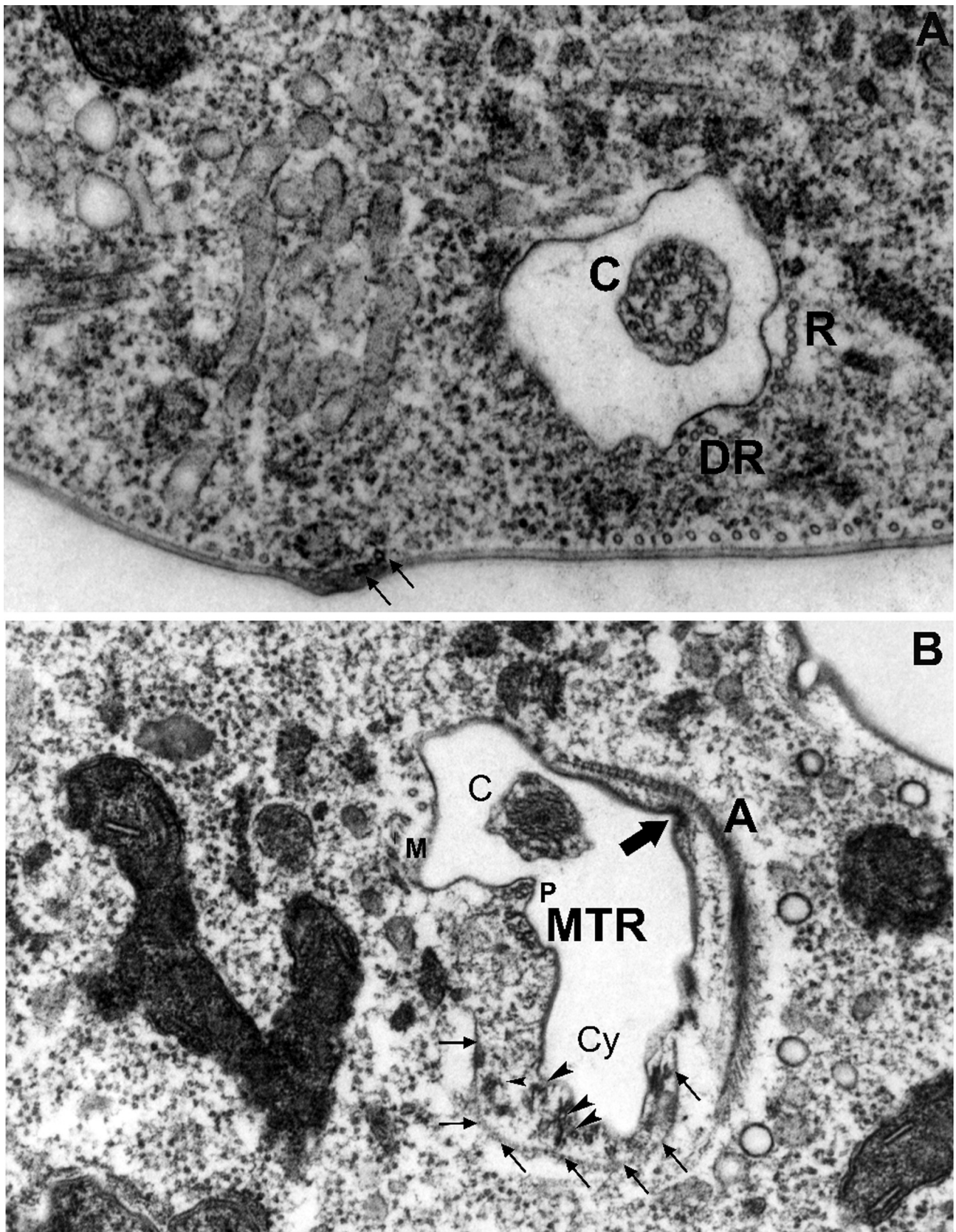
Fig. 4. Transmission electron micrographs of *Scytomonas saepesedens*. **A.** Transversely sectioned cilium (C) showing single central pair microtubule and simplified paraxonemal rod at that level. On the reservoir right is a band of eight evenly cross-linked mts plus two more widely spaced, probably collectively the dorsal row (R); and a band of three mts, possibly the dorsal root (DR), and some single mts to its left.
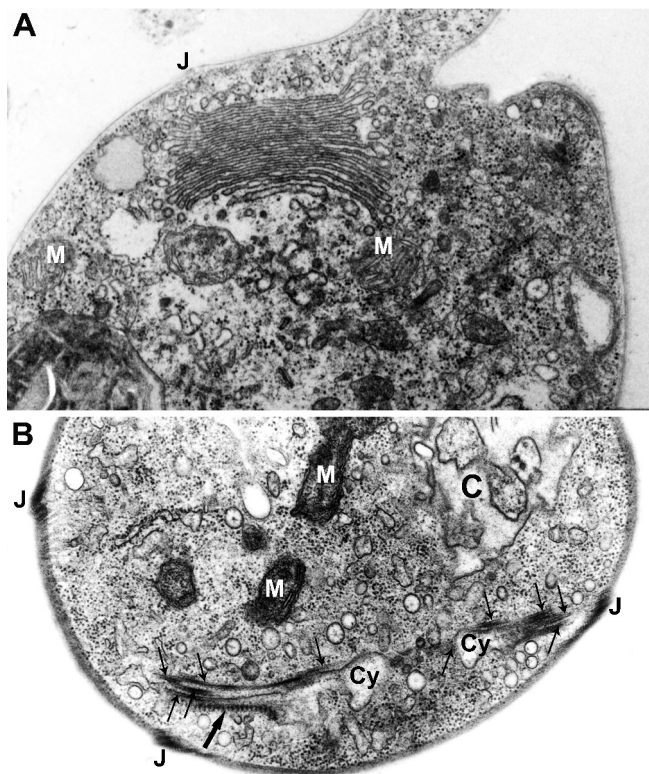
Fig. 5. Transmission electron micrographs of *Scytomonas saepesedens*. **A.** Highly-stacked Golgi complex with associated multivesicular body and discicristate mitochondrion (M). **B.** cytopharyngeal region; grazing section through the side of the cytopharynx (Cy) shows membranes, associated reinforced microtubules (small arrows) and a membrane-associated dense periodic structure (large arrow). Three dense thickened strip joints (J) are visible; about 14 obliquely sectioned microtubules are just below the left one, at least five more at each of the others. C = ciliary pocket.

ciliary cleft consists of two dense arcs, the inner bearing about eight dense teeth at one end on its concave face (Fig. 8). The ciliary cleft has a narrow basal curved extension associated with several dense patches of undetermined structure (Fig. 8).

The 10 longitudinal pellicular strips are of approximately equal width; the three making up most of the ventral surface are somewhat wider than the four forming the dorsal surface (Fig. 7A); these seven upper and lower strips are predominantly flat or slightly concave, only the edge strips of the slightly flattened cell being obviously convex. At joints one
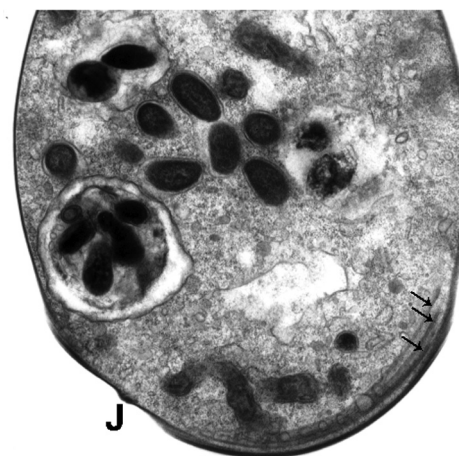

Fig. 6. Transmission electron micrograph of *Scytomonas saepesedens*. About five microtubules underlie the pimple-like strip joint (J). The curved vesicle-associated cytopharynx shows three reinforced microtubules (arrows); a branched discicristate mitochondrion is adjacent. Numerous rod bacteria are within cytoplasmic vacuoles.

strip overlaps the other, the outer part being cusp-like with a pointed apex in cross section. One broad longitudinal band of 8–13 mts underlies the inner part of each strip, occupying nearly half its width at the joint edge (on its right dorsally: Fig. 8). Numerous tubular extrusomes are on either side of the ciliary cleft and alongside the FA (Fig. 8). Mitochondria are discicristate. Food vacuoles indicate phagotrophic feeding on bacteria. Cysts have a thick tripartite wall; projections form the outermost dense layer (Fig. 7C)

Morphology of *Entosiphon oblongum*

Entosiphon oblongum differs in shape from the original *Entosiphon sulcatum* (Ritter von Stein 1878), being oblong not ovoid (Fig. 1J–S). It closely resembles the oblong flagellate identified as *E. sulcatum* by Lemmerman (1913), suggesting excessive past lumping (see Taxonomy section). Because of its shape it was initially taken for a *Ploeotia*, but careful study showed that its siphon is extensible but less obviously (Fig. 1K–N, Q–S) than in *E. sulcatum*. Moreover it has the three rods characteristic of the siphon (Fig. 1M, O, R, S); only two are present in the FA of *Ploeotia vitrea*, *Decastava*, *Keelungia*, and *Serpenomonas*.

Two densely stained mts (arrows) each with about four short projections closely underlie the heel of the right strip beside the thickened strip joint. The right pellicular strip is closely underlain by 12 mts without obvious linkers and the left one by about three, more widely spaced; right and left describe these micrographs, with no implications of absolute orientation (A and B are viewed from opposite directions, so left and right are inverted, and also somewhat mutually rotated). **B.** Section through the cytostome region, closer to the centriole, through ciliary transition zone with much dense material within the outer doublets and several dense regions outside them but no discrete paraxonemal rod. The most conspicuous oral support is a broad curved fibrous sheet (A) to the right of the reservoir; slenderer inner microfibrillar arc (thin arrows) curves round a region containing dense fibrillar structures and mts (arrowheads). Four or five reinforced mts (MTR) are adjacent to a pair of mts (P) that support the ridge delimiting the cytostomal region (Cy) from the ciliary pocket (c). Dense material links the groove delimiting the other end of the cytostome region (thick arrow) to the outer fibrillar arc. A band of three microtubules (M, probably the dorsal root) has two adjacent single mts nearby (possibly two dorsal row pellicle mts extend more deeply into the reservoir than others). A coated pit is on the cell surface and several large coated vesicles with pale interiors are to the right of the fibrous sheet.
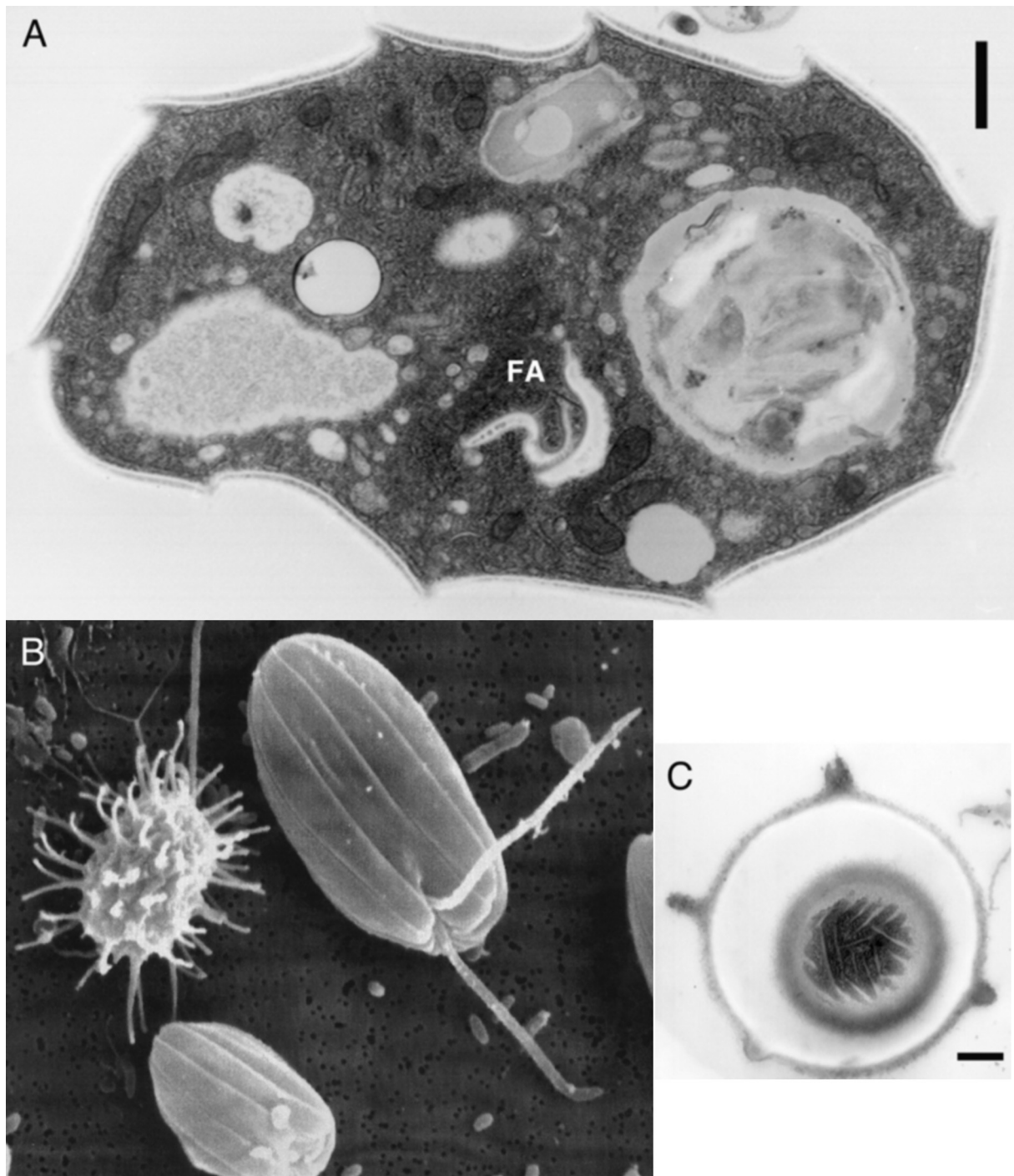
Fig. 7. Electron micrographs of *Decastava edaphica*. **A.** Transmission electron micrograph (TEM) sectioning the feeding apparatus (FA) roughly transversely where the rods are not obvious; note the cusp-like strip joints and that ventral strips (lower) are slightly broader than dorsal ones (upper). Viewed from rear of cell; ventral strip overlaps point to right. Scale bar 1.1 μm. **B.** Scanning electron micrograph in ventral view showing posterior cilium emerging from short ventral groove and broad pellicular strips without marked sutural ridges; micrograph taken before the culture became uniprotist – the amoeboflagellate on the left bristling with haptopodia is the cercozoan *Aurigamonas solis*. **C.** TEM of cyst showing multilayered wall with projections and pellicular ridges near one end of the cell. Scale bar 0.6 μm.

Euglenoid molecular phylogeny

Hsp90 groups *Scytomonas* with *Petalomonas cantuscyngi* as a maximally supported petalomonad clade (Fig. 9); this branch is longer than any others in Euglenozoa, showing accelerated evolution, but consistently groups with *Decastava* as a weakly supported stavomonad clade. This proves that *Scytomonas* is secondarily uniciliate. Petalomonads were
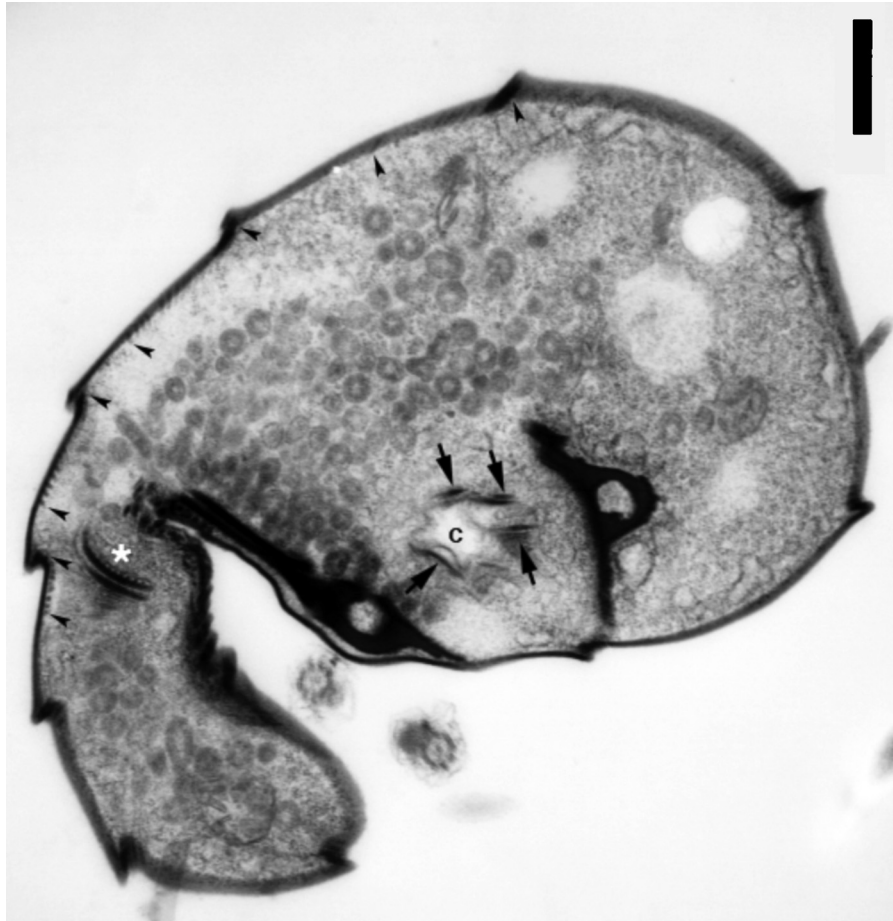
Fig. 8. Transmission electron micrograph of *Decastava edaphica* in TS through apical end. Shows two cilia emerging from the transversely oriented reservoir; two transversely sectioned hollow dense feeding rods with lateral flanges, that on left supporting the central, longest ventral pellicular strip; and vanes (arrows) associated with the cytopharnyx (C). The asterisk marks the dorsal feeding apparatus comb. Arrowheads show the approximate extent of the broad microtubular bands associated with the indented edge of the pellicular strips. Scale bar 1.1 μm.

never the deepest branching euglenoids. 18S rDNA trees (Fig. S1 and Cavalier-Smith 2016) robustly place *Scytomonas* as sister to an environmental sequence from Arctic sand (EF100248), jointly sister to *Petalomonas cantuscygni* plus a marine microbial mat sequence (CAT 0.94) or to *Petalomonas* alone (ML 52%); this *Scytomonas/Petalomonas* clade is robustly sister to another Arctic marine sand sequence (Fig. S1). That joint clade is maximally supported as sister to one comprising *Biundula* (=*Petalomonas*) *sphagnophila, Notosolenus urceolatus*, and four environmental sequences, this large clade being firmly sister to *Notosolenus ostium* as a petalomonad clade (0.99, 100% support).

Branching within Euglenozoa is identical for Hsp90 and 18S rDNA trees except for *Entosiphon*, whose rDNA sequences are so divergent from other Euglenozoa that they are very hard to align and invariably form the longest branch on the tree and appeared in six conflicting positions with different algorithms and taxon samples (Cavalier-Smith 2016). All trees group holophyletic Euglenophyceae (plastid-bearing) and heterotrophic Peranemea (ancestral to them) as a maximally or near-maximally supported clade, here called Spirocuta (Fig. 9) because of their spiral, often metabolic,

pellicle that contrasts with the invariably rigid longitudinal barrel stave-like pellicle of basal euglenoid lineages (*Entosiphon* plus Stavomonadea). Hsp90 and CAT rDNA trees that include Percolozoa in outgroups show *Entosiphon* as the most divergent euglenoid, sister to all others (Fig. 9; and Cavalier-Smith 2016 for additional trees using the present comprehensive alignment); most other trees put *Entosiphon* as sister to stavomonads or to *Keelungia* only: one CAT tree put them as sister to the *Ploeotia*/Spirocuta clade, another as sister to Spirocuta only; one ML tree, clearly artefactually, put them as sister to Postgaardea (Cavalier-Smith 2016). No rDNA position for *Entosiphon* has strong support, but all contradict earlier inclusion of *Entosiphon* in Peranemida (Cavalier-Smith 1993b), as does Hsp90 strongly. In most cases, inclusion of *Entosiphon* or not did not alter tree topology, just support values for deepest euglenoid branches.

The *Entosiphon oblongum* sequence is almost identical to one (AY425008) from an *Entosiphon* clone we previously isolated from South African soil, but did not regard as *E. sulcatum* as its FA was not obviously protrusible (von der Heyden et al. 2004). These two sequences almost certainly represent the same species and are quite distinct (about 96

Fig. 9. PhyloBayes CAT-GTR-GAMMA tree for Hsp90 of euglenoids and other eukaryotes (696 amino acid positions). Newly sequenced taxa are in bold. Support values for bipartitions are posterior probabilities (left) and bootstrap percentages for 100 fast bootstraps for a separate RAxML gamma LGF analysis for the same alignment (right). Black blobs mean maximal (1.0, 100%) support by both methods. Taxa for some outgroups whose internal phylogeny is irrelevant to this paper are collapsed to enable fitting onto one page; the number of species for each is shown beside its group name. The tree is rooted according to Cavalier-Smith (2010, 2013, 2014b) and has the largest taxon sample to date (297 species); support for basal euglenozoan branching is much higher than for neokaryotes.

systematic differences) from the two sequences (almost identical) of the CCAP *E.* '*sulcatum*' strains, and from a third partial sequence from activated sludge that probably represents a third *Entosiphon* species. Apart from three differences at the beginning and two at the end of the molecule there are only 16 internal nucleotide differences between *E. oblongum* and AY425008, several of which appear to be incorrectly called numbers of repeated nucleotides in AY425008, an error to which ABI software is prone. Though there may be a few genuine differences we can now reasonably identify the South African strain as *E. oblongum* also; as von der Heyden et al. (2004) did not video it, we would have overlooked its very slight mouthpart protrusion. The Hsp90 sequence of *Entosiphon oblongum* is clearly more obviously different from that of *E. sulcatum* (Fig. 9), confirming that they are separate species. For both *Entosiphon* Hsp90 is conservative and forms a short branch on the tree that is the deepest branching within Euglenozoa, and never shows any tendency to group with *Peranema*, with which it was formerly classified.

Except for the position of *Entosiphon*, nearly all features of the euglenoid part of the tree were the same for both methods with all eight alignments. Notably, *Ploeotia* cf. *vitrea* never groups with Stavomonadea, suggesting that *Decastava*, *Keelungia*, and *Serpenomonas costata* are rightly excluded from *Ploeotia* (see also Cavalier-Smith 2016). Instead *P.* cf. *vitrea* is sister to Spirocuta, the robust clade comprising subclades Peranemida, Anisonemia, *Teloprocta* and Euglenophyceae. This contradicts a previous study placing *P.* cf. *vitrea* (no significant support) below the last common ancestor of all other Euglenozoa plus postgaardeans (Lax and Simpson 2013). When *Entosiphon* is excluded from the analyses, *Decastava* and *Keelungia* are significantly, sometimes strongly, supported sisters (clade Decastavida); this relationship persists if *Entosiphon* is added except in samples where *Entosiphon* is sister to *Keelungia* (Cavalier-Smith 2016). Except when *Entosiphon* thus intrudes, Stavomonadea is a clade with stronger CAT than ML support. In the absence of *Entosiphon*, Petalomonadida is sister to Decastavida on CAT trees, and *Serpenomonas* the deepest-branching stavomonad; with ML Decastavida can be sister to Petalomonadida (Fig. 9) or to *Serpenomonas* depending on taxon/sequence sample, both alternatives insignificantly supported. The marked separation of *Serpenomonas* from Decastavida and *Ploeotia* is consistent with its radically different pellicle consisting of alternating broad and and narrow stave-like strips. To reflect its unique pellicle morphology amongst euglenoids and deep phylogenetic separation from all other orders, *Serpenomonas* is now put in new order Heterostavida (Cavalier-Smith 2016).

Entosiphon was never sister to Petalomonadida, unlike some previous rDNA trees (Lax and Simpson 2013). As *Entosiphon* can appear in at least seven different places on 18S rDNA trees, they are almost useless for placing it relative to other euglenoids without independent evidence to interpret them. As Cavalier-Smith (2016) explains, Hsp90 and comparative anatomy agree in strongly showing *Entosiphon* to be the sister to all other euglenoids (Fig. 9). This is

consistent with ML being often less accurate (Cavalier-Smith 2015) and other alignments having too little information for CAT to be accurate, and with our view that it is best to include as many positions and taxa as practicable (by making more alignment effort than is usual), use a more broadly representative outgroup than is usual, and a heterogeneous model for 18S rDNA trees for difficult cases (Cavalier-Smith 2014a).

Spirocuta show one significant difference from the previously most comprehensive euglenoid tree (Lax and Simpson 2013): *Dinema* do not group together; *Dinema platysomum* alone is sister to *Anisonema*, but *Dinema sulcatum* branches one node more deeply as their sister; this paraphyly is usually weakly supported. Our trees are slightly contradictory concerning *Dinema/Anisonema* (new order Anisonemida: Cavalier-Smith 2016), previously an insignificantly supported clade (Lax and Simpson 2013); all 8 of our best ML trees show Anisonemida as a clade (49–75% BS) as on Fig. S1, as do five of 8 CAT trees (0.59–0.89), but it was paraphyletic on three CAT trees as *Dinema sulcatum* branched even deeper below other anisonemids plus natomonads (Fig. 9 plus both CAT trees using only 1425 positions but no Percolozoa); thus with CAT but not ML its holophyly is sensitive to taxon sampling. Our trees strongly confirm that two phagotrophs formerly misidentified as *Heteronema* never group together. *Neometanema* is invariably sister to osmotrophic Rhabdomonadina (forming clade Natomonadida with near maximal PP and insignificant BS support). However, *Teloprocta* (formerly *Heteronema*) *scaphurum* is either sister to the photosynthetic Euglenophyceae (12 of 16 trees) as Lax et al. (2013) and Lee and Simpson (2014a) found, or to Anisonemia (the clade comprising Natomonadida and Anisonemida; 3 trees) or (one ML tree only) sister to Rhabdomonadina (see Cavalier-Smith 2016 for details).

Hsp90 gene introns, possible RNA editing, and heterogeneity

Six independently sequenced clones of *Decastava edaphica* Hsp90 genes all had spliceosomal introns with typical splice junction sequences and lengths from 67 to 103 nucleotides (Table 1). In both *D. edaphica* and *Entosiphon oblongum* Hsp90 genes had multiple frameshifts that would result in truncated proteins with incorrect C-terminal amino acid sequences unless corrected either by insertional RNA editing or by translational frame-shifting. In *Decastava* six frameshifts could in principle be corrected by single nucleotide insertions after nucleotides 917 (inserting U), 924 (U), 953 (G), 974 (U or C), 978 (U, A, G or C), 999 (C). As these are highly clustered within 83 nucleotides, a single short guide RNA like that responsible for U-insertional editing in euglenozoan mitochondria could correct them all. All six independent clones of *Decastava* showed the same six frameshifts so they cannot be attributed to sequencing errors.

All six sequenced Hsp90 clones of *Decastava* had differences in nucleotide sequence at 24 positions: 23 single

Table 1. Intron positions and splice junction sequences for *Decastava edaphica* Hsp90 genes.

Intron 1 nucleotide positions 94–176 (length 80 nucleotides)
Intron 2 nucleotide positions 487–574 (length 88 nucleotides)
Intron 3 nucleotide positions 845–911 (length 67 nucleotides)
Intron 4 nucleotide positions 1086–1189 (length 104 nucleotides)
Intron 5 nucleotide positions 1702–1796 (length 95 nucleotides)

Exon 1/Intron 1 AGUGCUAC/CAUUGUGC Intron 1/Exon 2 UUUUCU**AG**/**A**UGGGAGU
Exon 2/Intron 2 AGGUACCA/CA**A**ACAUA Intron 2/Exon 3 AGGUCA**AG**/**G**AGGUGAG
Exon 3/Intron 3 UCAUCAU**G**/**G**GUGUGAC Intron 3/Exon 4 UGCUGUUA/**G**ACAAUGCG
Exon 4/Intron 4 ACAACAA**G**/**GU**GAUGGA Intron 4/Exon 5 UUUCGCAG/**G**AGGACUAC
Exon 5/Intron 5 GUCACA**AG**/**GU**AAGCGG Intron 5/Exon 6 CUUUUC**AG**/CGAGUAUGGC

Eight of the 10 splice junctions show putative relics (bold) of the ancestral junction AG/GU proposed as the protosplice sites into which introns originally inserted when spliceosomal introns originated from group II introns in the ancestral eukaryote (Cavalier-Smith, 1993a). The usual pyrimidine-rich cluster likely to represent the lariat branch site during intron excision is evident upstream of the 3′ splice junction in four introns.

Table 2. Heterogeneous sites in *Decastava edaphica* Hsp90 genes.

	exon 1					intron 1				
nucleotide position	9	12	21	27	71	96	120	134	161	173
clone 19	G	A	G	T	A	T	G	A	A	A
clone 20	A	G	T	C	A	G	T	A	A	T
clone 21	A	G	G	C	G	G	G	G	A	T
clone 22	G	G	G	C	A	G	G	A	A	T
clone 24	G	G	G	C	A	G	G	A	G	T
clone 23	G	G	G	T	A	G	G	A	A	T

Contd:

exon 2					intron 2		exon 3			exon 4	intron 4	exon 5	
298	303	308	321	334	530	572	579	631	809	1062	1199	1351	1584-7
T	G	**A**	G	A	G	A	T	T	A	T	A	G	GGA
C	G	**A**	**C**	A	A	A	T	T	A	T	A	G	GGA
C	A	G	G	**G**	G	A	A	T	A	**C**	A	G	-
T	A	G	G	A	G	A	T	T	A	T	**G**	G	-
T	G	G	G	A	G	T	T	C	A	T	A	G	GGA
T	A	G	G	A	A	A	T	T	**G**	T	A	A	GGA

7 substitutions changing the amino acid sequence from the canonical sequence of **clone 24** are in bold.

nucleotide substitutions and one three-nucleotide deletion that removes one lysine from a run of four (Table 2). The seven of these polymorphisms present in more than one clone cannot reasonably be sequencing errors. There is no reason to think that any are sequencing errors; two thirds of them do not change the amino acid sequence and those that do all do so at positions that are evolutionarily variable in euglenoids. We interpret them as natural genetic polymorphisms. Interestingly, 21 are clustered near the 5′ end of the gene (15 in the first 334 nucleotides: Table 2) and only two near the 3′ end with and only two in the major middle region between nucleotides 632–1350. No more than two alternative nucleotides were present at any one site. However, the multiply represented polymorphisms at positions 9, 27, 298, 303, 308, 530, 1584 occur in different combinations amongst the clones, suggesting intragenic recombination. The two independently cloned Hsp90 sequences of *Scytomonas* also show two single nucleotide differences near their 3′ end. Though

inspection of the sequence traces shows they are unambiguous, both are in a more conserved region and we cannot be sure they are not cloning or PCR errors; therefore we made a composite sequence for the Fig. 9 tree choosing the amino acid at both positions that matches its closest relatives.

Taxonomy

Entosiphon oblongum sp. n. Cavalier-Smith and Vickerman. **Syntypes:** illustration Fig. 1J–S; culture CCAP 1220/2; sequences GenBank 18S rDNA KP306754, Hsp90 KP306762. **Diagnosis:** Unlike *E. sulcatum* cell oblong not ovoid and siphon extends only about 1 μm not ∼2.5 μm; anterior more truncated than in *E. ovatum*, the most similar species. Cell length rather variable: 17–28 μm; width 5–8 μm; shorter than *E. sulcatum*, much longer than the broadly oval *E. applanatum* (13.5–19.5 μm: Preisig 1979), and still smaller marine *E. limenites* (Norris 1964:

12–15 µm). Unlike *E. sulcatum*, *polyaulax*, *limenites*, and *striatum*, which have prominent longitudinal strips, and to a lesser extent *E. ovatum*, strip pattern not evident by light microscopy. Anterior cilium projects one cell length, often basally straight and smoothly curved towards siphon side; straight, posterior gliding cilium projects 1/6 to ¼ cell length (3/4 in *E. ovatum*). **Etymology:** *oblongus* L. oblong, rather long. **Type locality:** soil, Falkland Palace garden, Scotland (KV).

Comment 1. This strain's 18S rDNA differs by 115 nucleotides from strain CCAP 1220/1A and 122 nucleotides from CCAP 1220/1B, both identified as *Entosiphon sulcatum*, and is clearly therefore a different species. However, as no light micrograph is available for the sequenced CCAP strains (Busse and Preisfeld 2003b) we do not know if they were correctly identified by their isolator E. A. George, though the two sequences are sufficiently similar (differing by 9 nucleotides) for them to be considered one species. We need more *Entosiphon* sequences supported by documented microscopic identification, as for *E. oblongum*. Micrographs of the *E. sulcatum* yielding the Hsp90 sequence (Breglia et al. 2007) are consistent with that strain being the same species as *A. sulcatum*, but insufficiently clear to show whether it had 10 or 12 strips (probably not 8 like Ritter von Stein's *E. sulcatum*).

Cooment 2. Frequent misidentification or overlumping of *Entosiphon sulcatum*: We do not agree with Ritter von Stein (1878) and most subsequent authors that his well-described *Entosiphon sulcatum* with posterior cilium projecting only about half a cell length is conspecific with *Anisonema sulcatum* of Dujardin (1841, who suggested it needed a separate genus), with posterior cilium projecting one body length and no siphon noted (but easily overlooked as microscopes were less good in 1841 than 1878). The two species differ greatly in cell length (*E. sulcatum* 31–45 µm; *A. sulcata* 22 µm), being similar only in shape and being furrowed, rigid, and biciliate and probably congeneric. They may differ also in pellicle strip number: Rittter von Stein showed 8 predivision and 4 postdivision strips on one side of the cell, implying that the unduplicated number was 8 in total, whereas Dujardin drew 5 strips on one side (implying 10 altogether). Later light microscopists noted 8 (Dangeard 1902), 6–12 (Lackey 1929) or 12 (Hollande 1942, 1952) strips in cells identified as *E. sulcatum*. Huber-Pestalozzi (1955) accepted *E. sulcatum* (Dujardin) Stein supposedly with 4–8 strips as a separate species from *E. ovatum* Stokes, 1885 with supposedly 10–12 (actually 10 **or** 12: Stokes 1888). Mignot (1967) argued that euglenoid species have a constant strip number and *E. sulcatum* really has 12, as in his own strain, even though that disagreed with both Dujardin and Ritter von Stein; he suggested other numbers were observational errors.

Different strains studied ultrastructurally have genuinely different strip numbers. Those of Belhadri and Brugerolle (1992; from D. J. Patterson) and Triemer (1988; from the Delaware/Raritan canal, New Brunswick, NJ, USA in spring 1985) both clearly show 10 old grooves/strips and 10 young ones in cells in cytokinesis, so both had 10 unduplicated strips. They could therefore be *A. sulcatum* of Dujardin, but not *E. sulcatum* of Ritter von Stein; yet one cannot be sure as neither paper had light micrographs of living cells. By contrast three other independently isolated strains (Mignot 1963; Solomon et al. 1987; Withold 2001) all had 12 strips, and probably therefore represent different undescribed species from those with 10. Supporting this are systematic qualitative differences in pellicle structure between the 10 and 12-strip strains. All three 12-strip strains have predominantly relatively shallow, broad grooves formed by 12 S-shaped pellicle strips; in one (Withold 2001) these are fairly equal dimensionally, and the pellicle of this strain resembles that of *Lentomonas*, which differs mainly by having a flattened ventral face (Farmer and Triemer 1994), more than do the other two (Mignot 1963; Solomon et al. 1987) whose grooves are heterogeneous in appearance with two separated by three strips being much deeper than others, suggesting that these 12-strip strains may represent two distinct species. By contrast the 10-strip strains generally have much deeper, narrower grooves that all (Triemer 1988) or mostly (Belhadri and Brugerolle) appear in transverse section (TS) as near-circular with only a very narrow opening overhung by strongly projecting lips that are absent in all 12-strip strains. The groove lips are asymmetric; in the Triemer strain the lip on one side bearing an obvious small subgroove making it appear very similar to the asymmetric bifurcate strip suture region of *Ploeotia vitrea* and *Serpenomonas costata*; that of Belhadri and Brugerolle has a similar but less obvious structure, as does one edge of each strip in the Witold and Mignot strains; even the Solomon et al. (1982) strain has weak densities that could be reduced versions of similar strip joints. The circular cross section grooves of the 10-strip *Entosiphon* therefore superficially resemble the circular cross section grooves of *Serpenomonas costata* (Farmer and Triemer 1988), but as *Serpenomonas* has aymmmetric fork structures on both lips this groove shape similarity is superficial convergence. Curiously, Triemer and Fritz (1987) Fig. 1 is an SEM seemingly with ∼12 strips from a culture isolated at the same time and place as the 10-strip one of Triemer (1988), suggesting that two different clones were involved (within a single culture or two) – Triemer and Farmer (1991b Fig. 17) show a different 12-strip cell. A third *E. 'sulcatum'* strain from the same locality apparently had 12 strips with alternate grooves differing systematically in depth (Leander and Farmer 2001 Figs 31, 32), unlike the rest, and may be yet another species. The most satisfactory solution on present evidence is to accept *Entosiphon sulcatum* as having 10 grooves and strips (Dujardin 1841) and establish new names for 8- or 12-strip species when supporting sequences are available (using *E. ovatum* for the most similar 12-strip strain). Hollande (1942) showed figures of chubby 'sulcatum' cells like those of Dujardin and Ritter von Stein apparently with 10 strips (Pl. X Figs 7,8) and another more elongate cell similar to *E. ovatum* cells with apparently 12 (Pl. X Fig. 8), so Mignot (1967) oversimplified in saying Hollande's observations 'confirm' 12;

even he unwittingly probably studied two species. *E.* 'sulcatum' drawn by Preisig (1979) was only 22 μm but was anteriorly more pointed and less truncated than *E. sulcatum* of Ritter von Stein and *E. oblongum*; it is morphologically more similar to *E. ovatum* (Stokes 1885, 1888: 25–28 μm) or a close relative. Lackey (1962) wrote that *Entosiphon cuneatiformis* 'bears little resemblance to the other five species of the genus'; it probably should be a new genus, as possibly should *E. planum* with a unique ventral groove (Christen 1959). *Entosiphon applanatum* Preisig is very distinct, but not the same as *Lentomonas* 'applanatum' of Farmer and Triemer (1994) (see Ekebom et al. 1995; Patterson and Simpson 1996; who showed that L. 'applanatum' was really *Ploeotia corrugata* Patterson and Simpson, 1990, renamed *Lentomonas corrugata* by Cavalier-Smith (2016)). *Entosiphon wrightianum* with two chromatophores (Woodhead and Tweed 1960) and apparently no cilia is not a euglenoid, possibly a green alga. In accord with the view that most flagellates named by Skvortzov are too inadequately described for reidentification (Patterson and Zölffel 1991) we did not compare *E. oblongum* with the 44 nominal *Entosiphon* species he named from 1957 to 1970 (listed by Larsen and Patterson 1990). As the genus may be over a billion years old (probably the oldest eukaryote genus) it could have speciated considerably.

New order Decastavida Cavalier-Smith.

Diagnosis: Posterior-cilium gliders with 10 longitudinal pellicular strips of approximately equal width, unlike *Serpenomonas*; strip joints smooth without projecting bifurcate ridges (unlike *Ploeotia*) or grooves (unlike *Serpenomonas*). Feeding apparatus with two dense hollow rods; dorsal jaw support strongly cemented; inner pharyngeal rod adjoining cytopharynx with prominent lateral dense flanges. **Etymol:** as for *Decastava*.

New family Decastavidae Cavalier-Smith. **Diagnosis:** eight or nine unreinforced microtubule pairs loop from dorsal jaw support to cytostome; outer rod with prominent flanges. Type genus:

Decastava gen. n. Cavalier-Smith. **Diagnosis:** 10 strip joints asymmetrically cusp-like in cross section with pointed non-bifurcate apex. Cytostome slit-like, separate from reservoir canal. Pharyngeal rods both with prominent lateral dense flanges, not just on the inner rod as in *Keelungia*, the one flanking the reservoir beginning more anteriorly and with very long inner flange. **Etymol:** *deca* – L. combining form of 10; *stave* E. from the resemblance of the strips to barrel staves (or Norwegian stave church planks). Type species *D. edaphica*:

Decastava edaphica sp. n. Cavalier-Smith and Vickerman. **Syntypes:** illustration Fig. 1F–I; culture CCAP 1265/2; sequences GenBank KP306753 (18S rDNA) KP306756-KP306761 (Hsp90). **Diagnosis:** Rigid ellipsoid biciliate gliding on posterior cilium projecting one third to under half a cell length; anterior cilium ∼10 μm beats spirally with strong kinks. Cells 12–13 μm long, ∼7 μm wide. Anterior dome-like connector(s) of feeding rod ∼1.7–2.3 μm wide, about ¼ to 1/3 body maximal width. Pharyngeal rods with a single

microtubule row facing eight vanes. **Similar species:** in LM like *Ploeotia* but no visible striations**. Etymology:** *edaphos* Gk ground, because from soil. **Type locality:** soil, Sourhope Scotland (KV).

Order Petalomonadida (Rigid cells without supporting rods or cemented oral supports; vanes present or absent; glide on anterior cilium). Family Scytomonadidae:

Scytomonas saepesedens sp. n. Cavalier-Smith and Vickerman. **Syntype:** illustration Fig. 1A–E; sequences GenBank 18S rDNA KP306755, Hsp90 KP306763–KP 306764. **Diagnosis:** Pyriform sedentary or gliding uniciliates; feed on bacteria via lashing cilium whilst cell attached basally to substratum more often than during gliding; also with dense granular rounded resting stage. Pellicle of 5 strips with smooth slightly dense sutures associated with cortical microtubule bands; no surface ridges or furrows; 8–14 μm long and 5–10 μm maximum width; single cilium ∼20 μm emerges from deep reservoir over half cell length; long transition zone with dense contents. Single contractile vacuole near base of ciliary pocket. **Type locality:** Horse manure, Scotland (isol. KV). **Etymology:** *saepe* L. often *sedens* L. sitting; because more often sedentary than gliding. **Comparisons with most similar species:** *Scytomonas pusilla* Rittter von Stein, 1878 was about 14 μm, with 20 μm cilium and essentially the same shape. *Copromonas subtilis* Dobell (1908) from frog gut was about 16 μm (range 7.5–20); though he studied it extensively in vivo he did not report sedentary feeding behaviour and it fed whilst gliding; unlike our strain cysts were sometimes seen, and its shape was never shown as pinched in concavely at the anterior end as in our strain (Fig. 1C–E). Lemmerman (1913) synonymized *C. subtilis* with *S. pusilla*, which has been widely accepted (e.g. Sandon 1927). However he overlooked that the nucleus of *Scytomonas pusilla* Ritter von Stein, 1878 was somewhat in the anterior half of the cell and that of *C. subtilis* in the posterior end. For that reason and because of the non-pinched-in anterior end of *C. subtilis* we reject the species synonymy, but they are probably congeneric, so we make a new combination *Scytomonas subtilis* (Dobell) comb. n. Cavalier-Smith. The strain identified as *S. pusilla* by Mignot (1961, 1962, 1966) was 12 μm × 6 μm; from its shape and tadpole gut habitat it was probably *S. subtilis*. Neither Mignot nor others who observed *S. pusilla* from soil (e.g. Sandon 1927) reported sedentary feeding behaviour as predominates in our strain. Therefore, and because our strain is somewhat smaller, especially under culture conditions in Oxford, we made it a new species. This distinction needs testing by sequencing other non-sedentary *pusilla*-like strains, as does the synonymisation of *Copromonas* by sequencing gut symbionts. *Petalomonas minuta* Hollande, 1942 6–10 (14) × 4–5 μm, with ventral groove, had cilium about the cell length or slightly longer; *Petalomonas poosilla* (replacement name for *P. pusilla* Skuja, 1948 required by ICZN: see Larsen and Patterson 1990; Patterson and Larsen 1992) was 5 × 2–3 μm, no surface structures visible, cilium ∼1.5 x cell length (Larsen and Patterson, 1990) [Tong 1997 gives 6–8 × 2.5–4.5 μm for this species].

New genus *Biundula* Cavalier-Smith. **Diagnosis:** heterotrophic phagotrophic euglenoids with single emergent anterior cilium. Differ from *Petalomonas* in dorsal and ventral surfaces both having 2–8 smooth undulations when seen in TS, which in most species show mirror symmetry about their broad axis (*Petalomonas* is asymmetric about this axis, often trigonal in cross section). Unlike *Petalomonas* and *Scytomonas*, pellicle appears continuous without obvious sutures between discrete longitudinal strips. Type species *Biundula sphagnophila* comb. n. Cavalier-Smith. Basionym *Petalomonas sphagnophila* Christen (1962 p. 174, 196). **Etymol:** *bi* – L. two; *undula* L. little wave, referring to undulating dorsal and ventral surfaces. **Other new combinations:** *Biundula sulcata* comb. n. Cavalier-Smith Basionym *Petalomonas sulcata* Stokes 1888; *Biundula sinica* comb. n. Cavalier-Smith Basionym *Petalomonas sinica* Skvortzow, 1929; *Biundula septemcarinata* comb. n. Cavalier-Smith Basionym *Petalomonas septacarinata* Shawhan and Jahn, 1947 (spelling changed to *septemcarinata* by Huber-Pestalozzi (1955); as that change **a**ppears to be in prevailing use (166 google hits; 3 for the original spelling) and Huber-Pestalozzi attributed it to Shawhan and Jahn (1947) we deem it a justified emendation under Article 33.2.3.1. of ICZN; that change complies with Article 60.8 of ICN for algae, fungi and plants, it seems valid under both codes). **Comment.** The type species *Petalomonas abscissa* (Dujardin 1841), originally described as *Cyclidium abscissa* but transferred to the new genus *Petalomonas* by Ritter von Stein (1878) is unstudied by TEM or sequencing. However, Shawhan and Jahn (1947) showed it has a flat ventral surface with two sharp dorsal longitudinal keels slightly offset to the cell's right when viewed from above, so the dorsoventrally asymmetric morphotype must be included in *Petalomonas* sensu stricto. The cells they studied were from freshwater and 22–28 μm, both agreeing with the type (Dujardin 1841) from Seine river water (27.5 μm). Though they depict a slight posterior indentation not seen by Dujardin, and the cilium is relatively a little shorter, these differences are insufficient to question their specific identity; if we regard Dujardin's figure as a mirror image of theirs the cell shape is otherwise virtually identical and two longitudinal markings that probably represent the dorsal keels are laterally slightly offset in precisely the same direction as in Dujardin and even the left and right margins of the cell are asymmetrically curved in the same way. That near identity contrasts with the left right symmetry of the figures of Ritter von Stein, also with a symmetric posterior truncation distinctly broader than in Dujardin and relatively less posterior narrowing of the lateral margins; moreover Ritter von Stein's cells are much larger (44 μm), so we do not consider them the same species. Marine cells misidentified by Larsen and Patterson (1990 figs 25a,b, 26b) as *P. abscissa* are much smaller (17 μm) and an even more different shape – about as broad as long, unlike the type figure of Dujardin or drawing of Shawhan and Jahn (1947), both about 1.9 times longer than broad. Moreover the marine cells had much more prominent posterior indentation and much more

asymmetric ridge arrangement: only a single prominent dorsal strongly curved ridge, very asymmetrically arranged on the cells left (not two almost straight subequal ridges slightly to the cells right), and the ventral surface is not flat but has a small left ventral keel below the dorsal ridge plus a central double ridge (keel). This marine species is neither *P. abscissa* nor the also wrongly lumped separate species of Ritter von Stein, but an undescribed species.

New family Teloproctidae Cavalier-Smith. **Diagnosis**: as for type genus *Teloprocta* gen. n. Cavalier-Smith. **Diagnosis**: Elongate cylindrical or spindle-shaped spirocutes with two long cilia, dorsal extended anteriorly, rigid basal region glides on surfaces. In the type species hook-like dorsal cilium with much thicker paraxonemal rod than other euglenoids captures prey, helped by a mucilaginous web, and guides it into the vestibule (Breglia et al. 2013); defaecates pellets though posterior cytoproct. Dorsal jaw support mostly less robust and cemented than in Peranema, without cemented anchor to reservoir canal, but its outer dense body is hypertrophied as an 'accessory rod'. 28 extremely thick equal-width pellicular strips. Four microtubule-attached vanes, two attached posteriorly to the rod surfaces and two to one side of deep posterior rod grooves; the other side of each groove has a supplementary vane not edged by a microtubule. Type species *Teloprocta scaphurum* Cavalier-Smith comb. n. Basionym *Heteronema scaphurum* (Skuja 1934 dated 1932). **Etymol:** *telos* Gk end, completion; *proctos* Gk anus, because of its terminal cytoproct.

Comment: *Heteronema* is an anisonemid. Dujardin (1841) defined *Heteronema* as having a much thicker posterior cilium held straight backwards during locomotion (attached to substratum and retractile). Its anterior cilium was thinner and undulatory and the pellicle obviously with spiral strips and contractile – essentially the same as his non-squirming *Anisonema* except for its contractile pellicle. Though he did not understand that the posterior cilium promoted active gliding, both genera were certainly posterior-gliding spirocutes. Saville Kent (1880–1882) properly placed both in the same family Anisonemidae (together with *Entosiphon*, removed by Cavalier-Smith (2016) to its own new family, and *Diplomastix*, which are not euglenoids, but likely a heterogeneous collection of probably unidentifiable sarcomonad Cercozoa). Yet all '*Heteronema*' species described since Dujardin (1841) have been either swimmers with equal thickness cilia that do not glide on either or else gliders on an anterior usually thicker cilium. All are certainly assigned to the wrong genus because of their profound ciliary differences from *H. marina*, and also because all have cytopharyngeal rods visible in the light microscope unlike either of Dujardin's genera. The type species *Heteronema marina* was 60 μm and identifiable if refound, contrary to one assertion (Larsen and Patterson 1990). Ritter von Stein (1878) initiated over a century of confusion by ignoring and omitting Dujardin's species and transferring two entirely different biciliate metabolic spirocute zooflagellates to *Heteronema*: *Astasia acus* Ehrenberg, 1838 an elongate

spindle-like cell with anterior gliding cilium, probably an undescribed genus of Acroglissida (new anterior-gliding peranemean order established by Cavalier-Smith (2016) for Teloproctidae); and pyriform cells he called *Heteronema globuliferum*. He regarded *H. globuliferum* as the same species as the globular *Trachelius globulifer* Ehr., which is not credible, and as the seemingly uniciliate pyriform *Peranema globulosum* Dujardin, 1841 – we doubt that too, as Dujardin should have seen the trailing cilium that in *H. globuliferum* projected behind the cell by two thirds of its length, if it had been present, even though the cell was only 15–20 μm; *P. globulosum* is probably a peranemid but unidentifiable to species; *H. globuliferum* is either a peranemid or more likely an acroglissid, but not a *Heteronema* or anisonemid. We think all non-gliding 'Heteronema' belong in Natomonadida (a new non-gliding order established by Cavalier-Smith (2016) for the clade comprising *Neometanema* plus rhabdomonads), and most anterior ciliary gliders in Acroglissida, though some might be peranemids.

Discussion

Euglenoid genetic and population structure

Our finding considerable genetic heterogeneity in Hsp90 genes of *Decastava* is potentially significant in relation to the unknown population structure of euglenoids. Some heterogeneity might simply be because the studied culture may not have been strictly clonal. Probably some is a sign of multiple Hsp90 copies per nucleus through diploidy, polyploidy, or gene duplication. One expects initial divergence of multiple copies to be randomly distributed along the gene; its strong concentration at one end suggests secondary homogenization or concerted evolution, well known for multicopy rDNA where it can be partial rather than complete (e.g. Galián et al., 2014) but seemingly not seen before for Hsp90. Gene conversion, an homologous recombination mechanism more frequent than crossing over, can partially homogenise divergent multicopy genes (Chen et al. 2007) and probably exists in all organisms. The observed pattern is explicable by asymmetric conversion starting from near the 5′ end of the gene and extending towards the 3′ end but not all the way; if a hotspot for the double-strand breaks that initiate gene conversion existed in intron 3, conversion tracts needed to explain absence of polymorphism in the middle part of the gene would be several hundred nucleotides long – shorter than usual for yeast but longer than usual in mammals (Chen et al. 2007).

Spliceosomal introns are scarce in Euglenozoa (Breglia et al. 2007) as are group I introns (Busse and Preisfeld 2003a). The five spliceosomal introns in *Decastava edaphica* are the first for Stavomonadea and the second case for euglenozoan Hsp90 genes. Most have sequence signatures for typical spliceosomal introns, not atypical ones as were two of the three introns in *Peranema* (Breglia et al. 2007). None corresponds in position to any of *Peranema*; those of *Decastava*

are all short (67–104 nucleotides) as is typical of protists, but not ultrashort like those of *Peranema* that in that respect closely resemble the tiny introns of *Bigelowiella* nucleomorphs (Gilson et al. 2006). Their presence in Stavomonadea fits the view that such introns were probably abundant in early Euglenozoa and all eukaryotes and their virtual absence in kinetoplastids is secondary (Cavalier-Smith 1993a).

Our putative evidence for frameshifts in all sequenced *Decastava* and *Entosiphon* Hsp90 genes is probably the first, albeit indirect, evidence for insertional RNA editing in nuclear genes of Euglenozoa. For more direct evidence for editing, Hsp90 mRNA needs to be sequenced to test whether editing not cotranslational frame-shifting is how these euglenoids make Hsp90 genes translatable. Editing by U insertion is rampant in kinetoplastid mitochondrial genes, probably evolving as a rescue mechanism from a potentially harmful class of mutations (Cavalier-Smith 1993a; Covello and Gray 1993). Nuclear insertional RNA editing is rare, but U insertion occurs in humans (Zougman et al. 2008). The putative nuclear editing in euglenoids deduced here from the observed frameshifts seems able to insert any of the four nucleotides; it is yet another instance of neutral genome evolution (Cavalier-Smith 1993a) that probably evolved independently in euglenoids. Insertional editing may have evolved independently in early euglenozoan nuclei and mitochondria, though some editing machinery components might have been shared in early euglenozoan history.

Diversity of terrestrial phagotrophic euglenoids

Phagotrophic euglenoids are one of the four or five most speciose zooflagellate groups in soil. When reviewing soil flagellates, Foissner (1991) noted to his surprise that as many as 55 euglenoid species were recorded – 22 photosynthetic, 6 osmotrophic, and 27 phagotrophic – more than for phagotrophic chrysomonads (24) and nearly as many as for kinetoplastids (34), then seemingly the most speciose phagotrophic soil flagellates. Since then known terrestrial cercomonads have risen from 10 to 61 species (Bass et al. 2009; Howe et al. 2011a, including those from soil (predominantly), leaves and dung) and those of glissomonads from 4 to 41, so both cercozoan groups now surpass the currently known diversity of soil euglenoids or kinetoplastids (Howe et al. 2009, 2011a, 2011b). Thus most soil zooflagellates are Euglenozoa or Cercozoa. Our three new non-marine species increase terrestrial euglenoid phagotrophs to 30, showing that euglenoid terrestrial biodiversity is still poorly known; probably many more remain to be described. Many novel euglenoids have been described from marine habitats (Larsen 1987; Larsen and Patterson 1990; Lee 2008), but rarely characterised by electron microscopy or sequencing (Chan et al. 2013). These, as well as soil euglenoids, need more study by clonal culturing, essential for thoroughly investigating species boundaries, as established here between *Entosiphon sulcatum* and *oblongum*.

Scytomonas pusilla is by far the most frequently reported soil euglenoid (27 records: Foissner 1991). With so few characters it could really be numerous genetically distinct strains comprising several or many separate species, just as we found for the similarly morphologically undistinguished and overlumped '*Heteromita globosa*', really dozens of species (Howe et al. 2009) and recorded even more frequently (40 records in Foissner 1991). We therefore treated *S. saepesedens* as a new species because of its unique feeding mode, though it is otherwise distinguishable from *S. pusilla* only by being generally smaller. In the past it has been common to stretch original size limits for *Scytomonas* to avoid describing new species (e.g. Bicudo and Bicudo 1987), which is undesirable as it leads to drift in meaning of species names, excessively broad species, and lack of precision in reidentification later.

Scytomonas is secondarily uniciliate

Our trees show *Scytomonas* to be closely related to *Petalomonas* and nested so shallowly within euglenoids that its ancestors must have had two centrioles like all other Euglenozoa. We conclude that *Scytomonas* with a single centriole and cilium did not diverge early in euglenoid evolution (Cavalier-Smith 2010) but is a relatively recent simplification within Petalomonadida that evolved by losing the ventral cilium, centriole, and its roots. Mignot (1961) showed that the cilium regresses before mitosis and two equal new ones grow simultaneously during division, implying that the sole cilium is first generation – expected to have one centriolar root, possibly represented by an observed 3-mt band. For such uniciliate eukaryotes with a younger cilium, there is no general rule whether the centriole persists after the ciliary shaft regresses (e.g. *Monomastix, Pseudopedinlla* (Heimann et al 1989)) or not (e.g. *Phalansterium* (Hibberd 1983); probably *Scytomonas saepesedens*), so it has no great evolutionary significance whether a barren centriole or centriole vestige remains or not; in principle complete dissassembly is more economic unless retention is beneficial for attaching other structures (Cavalier-Smith 2013). Nonetheless, loss of the second centriole and presence of sex in *Scytomonas* (Mignot 1962) (both unknown in other euglenoids, and in all Euglenozoa except trypanosomatids, whose simpler pellicles could make pellicular recovery from syngamy easier) merit retaining its generic distinction from *Petalomonas*. But neither these nor the modest genetic distance from *P. cantsuscygni* on rDNA and to a lesser extent Hsp90 trees support keeping separate families, so we made younger Petalomonadidae a synonym of Scytomonadidae. Unfortunately we got no TS of its cytostome, so although rods are clearly absent we cannot be sure whether vanes are present as Mignot (1966) thought in *Scytomonas pusilla*, *Calycimonas*, and *Petalomonas*, or absent as Triemer and Farmer (1991a,b) assumed for *P. cantuscygni* and *Calycimonas robusta*. Uniciliate *Biundula* and *Petalomonas* sensu stricto nest independently within a biciliate paraphyletic *Notosolenus*, so *Biundula* lost the posterior cilium independently of *Scytomonas*.

Pellicle structure in *Scytomonas* and other petalomonads

Pellicular fold patterns seen in TS in *Petalomonas* are too varied (Huber-Pestalozzi 1955; Larsen and Patterson 1990; Shawhan and Jahn 1947) for all to be in one genus. They comprise two main contrasting groups: a minority whose dorsal and ventral surfaces both have 2–8 smooth undulations, that in most species show mirror symmetry about their broad axis, and a majority that are dorsoventrally asymmetric – typically flat or nearly so and bowed upwards dorsally often with 1–6 (most often 1–3) very prominent ridges. As the type species *P. abscissa* (Dujardin) Ritter von Stein is ventrally flat and dorsally with two nearly straight prominent dorsal ridges we restricted *Petalomonas* to such dorsoventrally asymmetric species and transferred five species with symmetric dorsal and ventral undulated surfaces to a new genus *Biundula*. On Figs 9 and S1 *P. cantuscygni*, ventrally slightly concave and dorsally with six equally prominent ridges, groups closely with *Scytomonas*, whereas on Fig. S1 *Biundula sphagnophila* is much further away. This greater genetic distance is also consistent with *Biundula*'s continuous pellicular ultrastructure, not obviously subdivided into strips (tiny dense spots at each pellicular ridge suggest that it may nonethelesss have a cryptic strip structure). By contrast in *Scytomonas* and *P. cantuscyni* one can detect very similar strip joints – in TS they appear as slightly dense pimples where adjacent strips abut with two mts associated with one strip edge. *Notosolenus urceolatus* has eight strips underlain by numerous mts and separated by shallow grooves at the crest of each longitudinal ridge (Lee and Simpson 2014b); as in all stavomonads strip edges abut rather than overlap. These flush strip joints distinguish these three genera from all spirocute euglenoids, where adjacent strips overlap (imbricate) (Leander and Farmer 2001). This contrast is also seen in hulls of wooden ships; in nautical terminology *Scytomonas*, *Notosolenus urceolatus*, *P. cantsuscygni*, and *Biundula sphagnicola* are carvel built with flush strips, whereas Spirocuta are clinker built of overlapping strips. Close inspection of Fig. 4A suggests that the *Scytomonas* joint is not totally symmetric, like a simple butt joint as usual in carvel construction, but is a stronger shiplap joint as used in timber cladding: strip edges at the suture seem flanged, the two mirror-image flanges overlapping exactly as in a shiplap timber joint.

Leander et al. (2001) asserted that *Petalomonas mediocanellata* has no strips, implying a continuous pellicle as in fiberglass hulls or monocoque racing cars. However, that conclusion was based soley on SEM, which we show does not reveal the five *Scytomonas* strips. Even in *P. mediocanellata* Fig. 1 of Leander et al. (2001) hints at three strips on one side of the cell, suggesting that it actually has five, just

like *Scytomonas*. The moncoque idea is directly refuted by earlier TEMs of *P. mediocannellata* (Farmer and Triemer 1988b) showing denser pellicle strip regions associated with more densely staining mts that look so similar to *Scytomonas* strip joints that they probably are butted/shiplap joints: two obliquely in their Figs 18 and 19 and three transversely in their Fig. 20 (where two show microdimples like reduced versions of the *Notosolenus* microgroove). Two nominal *Petalomonas* (*involuta* Skuja, 1939; *klinostoma* Skuja, 1948) have smooth unridged/non-undulating dorsal and ventral surfaces, but a deep lateral groove along the cell's left side. Almost certainly they are neither *Petalomonas* nor *Biundula*, but an undescribed genus that cannot be established without ultrastructure and/or sequences. In *Notosolenus ostium* (sequenced twice independently) ventral pellicular strips are visible under DIC (Larsen and Patterson 1990). It is evolutionarily unlikely that any euglenoids have a truly continuous monocoque pellicle; direct conversion from carvel to clinker is mechanistically more comprehensible than to monocoque.

Petalomonad FA simplification

The two unusual fibrous cytostomal arcs in *Scytomonas* are the first evidence for a petalomonad cytostomal skeleton. We suggest they are homologues of microfibrillar cores associated with two microtubule bands found in the *Diplonema* FA (the large PMB and second smaller unnamed arc: Montegut-Felkner and Triemer 1994) that we suggest were present in the diplonemid/euglenoid common ancestor; if that is correct ancestral petalomonads lost the associated cement at the same time as the cemented rods. The more robust outer arc may have some obliquely sectioned associated mts in Fig. 4B and is positionally appropriate for a PMB homologue. The slenderer inner arc seems to embrace a disordered mass of fibrillar material and microtubules, which could include MTR and PML mts (two additional distinct mt bands in *Diplonema* FA: Montegut-Felkner and Triemer 1994), making it positionally equivalent to a component of the feeding comb of *Serpenomonas* (Linton and Triemer 1999) and *Keelungia* (Chan et al. 2013) as Cavalier-Smith (unpublished) will explain in detail elsewhere. By making the cytostome smaller and losing cement petalomonads lost the clear distinction between rod apparatus and comb so obvious in other stavomonads. From their position within stavomonads on our trees, they clearly lost both mouthpart and rod cement; its absence cannot be the ancestral state for euglenoids. *Scytomonas* FA resembles that of *Calycimonas* (Triemer and Farmer 1991a, 1991b) in having a dense periodic supporting material arranged in an arc near the cytostome, with no close similarity to mature FA structures of non-petalomonad stavomonads or to mature *Entosiphon* FA. It is however remarkably like a similar arc alongside the reservoir that forms the core of early developing *Entosiphon* FA before cement deposition (Belhadri and Brugerolle 1992 Figs 8,9; compare with Figs 7 and 19 of *Calycimonas* in Triemer and Farmer 1991a,b); in both the

dense arc is delimited by a ridge on each side containing separate dense structures (simple dense band in *Calycimonas*; more complex groove-associated structures in *Entosiphon*); a conspicuous row of widely spaced mts extends away from both lateral membrane-linked densities in *Entosiphon* and from one in *Calycimonas*.

In *Calycimonas* on the other side of the cytopharynx from the widely spaced mt row is a double ridge behind which are disordered dense fibrillar structures and mts showing characteristics of MTRs, PML and also the ventral root; we suggest that this is equivalent to the double ridge beside the *Scytomonas* cilium in Fig. 4B containing putative MTR and PML. The structures lying between the minor fibrous arc and a double membrane projection of *Scytomonas* (Fig. 4B) are ultrastructurally similar and positioned identically to those lying behind the *Calycimonas* dense-arc-delimiting ridge that is not associated with the widely spaced mts; we suggest that both include MTRs and PML mts that loop over from those in the other ridge, and that the *Scytomonas* and *Calycimonas* FA are fundamentally similar. The major difference is that *Scytomonas* having lost the posterior cilium has no ventral or intermediate root, unlike biciliate *Calycimonas*; if correct, this gives further evidence that the MTR is fundamentally distinct from the ventral root even though in *Calycimonas* they are fairly close (two of three putative PML mt pairs are closer in *Calycimonas* to the ventral root than are the MTRs). Our inference of MTR/PML looping between ciliary and feeding pockets in the petalomonads *Calycimonas* and *Scytomonas*, as well as *Entosiphon*, is strongly supported in *Notosolenus urceolatus* where the whole loop can be directly seen in very few sections (Lee and Simpson 2014a): tentatively we suggest it has looping MTRs 1–5; whether it also retains one PML pair is unclear. As petalomonads retain MTRs, which carry vanes in other euglenoids it is unsurprising that one *Petalomonas* also retains four vanes (Mignot 1966).

Calycimonas and *Notosolenus* are respectively much more weakly and more strongly stained than *Scytomonas*' weakly stained fibrous arc, making it harder for opposite reasons to decide if they also have the two fibrous non-membrane linked arcs we found in *Scytomonas*. However, the curving widely spaced mt row in *Calycimonas* is associated with microfibrillar material that may be related to that of the major putatively PMB *Scytomonas* arc. In diplonemids cemented arcs are often associated with similar shaped ER cisternae; possibly therefore the ER arc that subtends the *Calycimonas* dense membrane-supporting arc and associated putative MTRs is given its shape by a poorly stained slender microfibrillar arc. Dense staining of *Notosolenus* can easily hide two arcs; Figs 6B,C of Lee and Simpson (2014a) suggest that at least one such arc (whether PMB or comb-homologue is unclear) may be present, and their Fig. 6E suggests it may have a membrane-associated dense arc like other petalomonads. Skimpy data for *Petalomonas* (e.g. Farmer and Triemer 1988b; Triemer and Farmer 1991a,b) are less informative but do not contradict the idea that petalomonad FA are fundamentally similar and probably retain all mt and microfibrillar

components of other euglenoid FAs, except probably the widespread likely homologues of diplonemid EM (Montegut-Felkner and Triemer 1994), and differ from others primarily in loss of cement and therefore support rods. The cytostome lip in *Petalomonas*, though much slenderer by SEM than in other stavomonads (Triemer and Farmer 1991b), has a similar C-shaped form that must reflect a basically similar underlying slenderer skeleton.

Petalomonads are secondarily simplified

The petalomonad FA is apparently a neotenous or arrested development of the ancestral stavomonad FA, an idea testable by serial sectioning developing *Serpenomonas* or decastavid FA and comparative serial sectioning across petalomonads. Our trees show that the traditional view of petalomonads as the most primitive of all euglenoids (Pochman 1953; Triemer and Farmer 1991a,b; Cavalier-Smith 1993b, 1995; Leander et al. 2001) is wrong. Strip number reduction, frequent FA simplification, multiple transitions from clinker to carvel pellicles, and posterior ciliary losses in petalomonads might all be adaptions to cell miniaturisation associated with secondary specialization in bacterivory. As petalomonad differences from other stavomonads are secondary losses and fewer than once thought, there is no longer justification for retaining a separate class for them (Cavalier-Smith 1993b), so in a following paper Petalomonadida, Decastavida, and Heterostavida are grouped as new class Stavomonadea (Cavalier-Smith 2016), a robust 18S rDNA clade.

Acknowledgements

Appendix A. Supplementary data

Supplementary data associated with this article can be found, in the online version, at http://dx.doi.org/10.1016/j.ejop.2016.08.002.

References

Akiyoshi, B., Gull, K., 2013. Evolutionary cell biology of chromosome segregation: insights from trypanosomes. Open Biol. 3, 130023.

Bass, D., Howe, A.T., Mylnikov, A.P., Vickerman, K., Chao, E.E., Smallbone, J.E., Snell, J., Cabral Jr., C., Cavalier-Smith, T., 2009. Phylogeny and classification of Cercomonadidae: *Cercomonas*, *Eocercomonas*, *Paracercomonas*, and *Cavernomonas* gen. n. Protist 160, 483–521.

Belhadri, A., Brugerolle, G., 1992. Morphogenesis and ultrastructure of the feeding apparatus of *Entosiphon sulcatum*: an immunofluorescence and ultrastructural study. Protoplasma 168, 125–135.

Bicudo, C.E.M., Bicudo, D.C., 1987. Some new and rare Euglenophyce from the State of São Paulo, southern Brasil. Acta Bot. Bras. 1, 43–48.

Breglia, S.A., Slamovits, C.H., Leander, B.S., 2007. Phylogeny of phagotrophic euglenids (Euglenozoa) as inferred from Hsp90 gene sequences. J. Eukaryot. Microbiol. 54, 86–92.

Breglia, S.A., Yubuki, N., Hoppenrath, M., Leander, B.S., 2010. Ultrastructure and molecular phylogenetic position of a novel euglenozoan with extrusive episymbiotic bacteria: *Bihospites bacati* n. gen. et sp. (Symbiontida). BMC Microbiol. 10, 145.

Breglia, S.A., Yubuki, N., Leander, B.S., 2013. Ultrastructure and molecular phylogenetic position of *Heteronema scaphurum*: a eukaryovorous euglenid with a cytoproct. J. Eukaryot. Microbiol. 60, 107–120.

Busse, I., Preisfeld, A., 2003a. Discovery of a group I intron in the SSU rDNA of *Ploeotia costata* (Euglenozoa). Protist 154, 57–69.

Busse, I., Preisfeld, A., 2003b. Systematics of primary osmotrophic euglenids: a molecular approach to the phylogeny of *Distigma* and *Astasia* (Euglenozoa). Int. J. Syst. Evol. Microbiol. 53, 617–624.

Cavalier-Smith, T., 1981. Eukaryote kingdoms: seven or nine? BioSystems 14, 461–481.

Cavalier-Smith, T., 1993a. Evolution of the eukaryotic genome. In: Broda, P., Oliver, S.G., Sims, P.F.G. (Eds.), The Eukaryotic Genome. Cambridge University Press, pp. 333–385.

Cavalier-Smith, T., 1993b. Kingdom Protozoa and its 18 phyla. Microbiol. Rev. 57, 953–994.

Cavalier-Smith, T., 1995. Zooflagellate phylogeny and classification. Tsitologiia 37, 1010–1029.

Cavalier-Smith, T., 1998. A revised six-kingdom system of life. Biol. Rev. Camb. Philos. Soc. 73, 203–266.

Cavalier-Smith, T., 2003. The excavate protozoan phyla Metamonada Grassé emend. (Anaeromonadea, Parabasalia, *Carpediemonas*, Eopharyngia) and Loukozoa emend. (Jakobea, *Malawimonas*): their evolutionary affinities and new higher taxa. Int. J. Syst. Evol. Microbiol. 53, 1741–1758.

Cavalier-Smith, T., 2010. Kingdoms Protozoa and Chromista and the eozoan root of eukaryotes. Biol. Lett. 6, 342–345.

Cavalier-Smith, T., 2013. Early evolution of eukaryote feeding modes, cell structural diversity, and classification of the protozoan phyla Loukozoa, Sulcozoa, and Choanozoa. Eur. J. Protistol. 49, 115–178.

Cavalier-Smith, T., 2014a. Gregarine site-heterogeneous 18S rDNA trees, revision of gregarine higher classification, and the evolutionary diversification of Sporozoa. Eur. J. Protistol. 50, 472–495.

Cavalier-Smith, T., 2014b. The neomuran revolution and phagotrophic origin of eukaryotes and cilia in the light of intracellular coevolution and a revised tree of life. In: Keeling, P.J., Koonin, E.V. (Eds.), The Origin and Evolution of Eukaryotes. Cold Spring Harbor Perspectives Biol. Cold Spring Harbor, http://dx.doi.org/10.1101/cshperspect.a016006.

Cavalier-Smith, T., 2015. Mixed heterolobosean and novel gregarine lineage genes from culture ATCC 50646: rDNA and α-tubulin trees congruent for deep eukaryote phylogeny. Eur. J. Protistol. 51, 121–137.

Cavalier-Smith, T., 2016. Higher classification and phylogeny of Euglenozoa. Eur. J. Protistol. 56, 147–170.

Cavalier-Smith, T., Chao, E.E., Snell, E.A., Berney, C., Fiore-Donno, A.M., Lewis, R., 2014. Multigene eukaryote phylogeny reveals the likely protozoan ancestors of opisthokonts (animals, fungi, choanozoans) and Amoebozoa. Mol. Phylogen. Evol. 81, 71–85.

Cavalier-Smith, T., Chao, E.E., Lewis, R., 2016. 187-gene phylogeny of protozoan phylum Amoebozoa reveals a new class (Cutosea) of deep-branching, ultrastructurally unique, enveloped marine Lobosa, and clarifies amoeba evolution. Mol. Phylogen. Evol. 99, 275–296.

Chan, Y.F., Chiang, K.P., Chang, J., Moestrup, O., Chung, C.C., 2015. Strains of the morphospecies Ploeotia costata (Euglenozoa) isolated from the Western North Pacific (Taiwan) reveal substantial genetic differences. J. Eukaryot. Microbiol. 62, 318–326.

Chan, Y.F., Moestrup, O., Chang, J., 2013. On Keelungia pulex nov. gen. et nov. sp., a heterotrophic euglenoid flagellate that lacks pellicular plates (Euglenophyceae, Euglenida). Eur. J. Protistol. 49, 15–31.

Chen, J.M., Cooper, D.N., Chuzhanova, N., Ferec, C., Patrinos, G.P., 2007. Gene conversion: mechanisms, evolution and human disease. Nat. Rev. Genet. 8, 762–775.

Christen, H.R., 1959. New colorless Euglininae. J. Protozool. 6, 292–303.

Christen, H.R., 1962. Neue und wenig bekannte eugleninen und Volvocalen. Rev. Algologique, N. Serie 4, 162–202.

Covello, P.S., Gray, M.W., 1993. On the evolution of RNA editing. Trends Genet. 9, 265–268.

Dangeard, P.A., 1902. Recherches sur les Eugléniens. Le botaniste 8, 97–369.

De Jonckheere, J.F., Dive, D., Pussard, M., Vickerman, K., 1984. Willaertia magna gen. nov., sp. nov. (Vahlkampfiidae), a thermophilic amoeba found in different habitats. Protistologica 20, 5–13.

Derelle, R., Torruella, G., Klimes, V., Brinkmann, H., Kim, E., Vlcek, C., Lang, B.F., Elias, M., 2015. Bacterial proteins pinpoint a single eukaryotic root. Proc. Natl. Acad. Sci. U. S. A. 12, E693–E699, http://dx.doi.org/10.1073/pnas.1420657112.

Dujardin, F., 1841. Histoire naturelle des zoophytes infusoires. Roret, Paris.

Ekebom, J., Patterson, D.J., Vørs, N., 1995/6. Heterotrophic flagellates from coral reef sediments (Great Barrier Reef, Australia). Arch. Protistenk. 146, 251–272.

Farmer, M.A., Triemer, R.E., 1988b. Flagellar systems in the euglenoid flagellates. BioSystems 21, 283–291.

Farmer, M.A., Triemer, R.E., 1994. An ultrastructural study of Lentomonas applanatum. J. Euk. Microbiol. 41, 112–119.

Foissner, W., 1991. Diversity and ecology of soil flagellates. In: Patterson, D.J., Larsen, J. (Eds.), The Biology of Free-Living Heterotrophic Flagellates. Clarendon Press, Oxford, pp. 93–112.

Galián, J.A., Rosato, M., Rosselló, J.A., 2014. Partial sequence homogenization in the 5S multigene families may generate sequence chimeras and spurious results in phylogenetic reconstructions. Syst. Biol. 63, 219–230.

Gilson, P.R., Su, V., Slamovits, C.H., Reith, M., Keeling, P.J., McFadden, G.I., 2006. Complete nucleotide sequence of the chlorarachniophyte nucleomorph: nature's smallest nucleus. Proc. Natl. Acad. Sci. U. S. A. 103, 9566–97571.

Hegner, R.W., 1923. Observations and experiments on Euglenoidina in the digestive tract of frog and toad tadpoles. Biol. Bull. 45, 162–180.

Hibberd, D.J., 1983. Ultrastructure of the colonial colourless flagellate Phalansterium digitatum Stein (Phalansteriida ord. nov.) and Spongomonas uvella Stein (Spongomonadida ord. nov.). Protistologica 19, 523–535.

Heimann, K., Benting, J., Timmermann, S., Melkonian, M., 1989. The flagellar developmental cycle in algae: two types of flagellar development in uniflagellated algae. Protoplasma 153, 14–23.

Hollande, A., 1942. Étude cytologique et biologique de quelques flagellés libres. Arch. Zool. Exp. Gén. 83, 1–268.

Hollande, A., 1952. Classe des Eugléniens (Euglenoidina Bütschli, 1884). In: Grassé, P.-P. (Ed.), Traité de Zoologie. Masson, Paris, pp. 238–284.

Howe, A.T., Bass, D., Vickerman, K., Chao, E.E., Cavalier-Smith, T., 2009. Phylogeny, taxonomy, and astounding genetic diversity of Glissomonadida ord. nov., the dominant gliding zooflagellates in soil (Protozoa: Cercozoa). Protist 160, 159–189.

Howe, A.T., Bass, D., Scoble, J.M., Lewis, R., Vickerman, K., Arndt, H., Cavalier-Smith, T., 2011a. Novel cultured protists identify deep-branching environmental DNA clades of Cercozoa: new genera Tremula, Micrometopion, Minimassisteria, Nudifila, Peregrinia. Protist 162, 332–372.

Howe, A., Bass, D., Cavalier-Smith, T., 2011b. New genera, species and improved phylogeny of Glissomonadida (Cercozoa). Protist 162, 710–722.

Huber-Pestalozzi, G., 1955. Das Phytoplankton des Süsswassers; Systematic und Biologie. Euglenophyceen. Teil 4. E. Schweitzerbart'sche Verlagsbuchhandlung, Stuttgart.

Lackey, J.B., 1960. Calkinsia aureus gen. et sp. nov., a new marine euglenid. Trans. Am. Microsc. Soc. 79, 105–107.

Lackey, J.B., 1962. Three new colorless Euglenophyceae from marine situations. Arch. Mikrobiol. 42, 190–195.

Larsen, J., 1987. Algal studies of the Danish Wadden Sea. IV. A taxonomic study of interstitial euglenoid flagellates. Nordic J. Bot. 7, 589–607.

Larsen, J., Patterson, D.J., 1990. Some flagellates (Protista) from tropical marine sediments. J. Nat. Hist. 24, 801–937.

Lartillot, N., Philippe, H., 2004. A Bayesian mixture model for across-site heterogeneities in the amino-acid replacement process. Mol. Biol. Evol. 21, 1095–1109.

Lasek-Nesselquist, E., Gogarten, J.P., 2013. The effects of model choice and mitigating bias on the ribosomal tree of life. Mol. Phylogenet. Evol. 69, 17–38.

Lax, G., Simpson, A.G.B., 2013. Combining molecular data with classical morphology for uncultured phagotrophic euglenids (Excavata): a single-cell approach. J. Eukaryot. Microbiol. 60, 615–625.

Leander, B.S., Farmer, M.A., 2001. Comparative morphology of the euglenid pellicle. II. Diversity of strip substructure. J. Eukaryot. Microbiol. 48, 202–217.

Leander, B.S., Triemer, R.E., Farmer, M.A., 2001. Character evolution in heterotrophic euglenids. Eur. J. Protistol. 37, 337–356.

Lee, W.J., 2008. Free-living heterotrophic euglenids from marine sediments of the Gippsland Basin, southeastern Australia. Mar. Biol. Res. 4, 333–349.

Lee, W.J., Simpson, A.G.B., 2014a. Morphological and molecular characterisation of Notosolenus urceolatus Larsen and Patterson 1990, a member of an understudied deep-branching euglenid group (petalomonads). J. Eukaryot. Microbiol. 61, 463–479.

Lee, W.J., Simpson, A.G.B., 2014b. Ultrastructure and molecular phylogenetic position of Neometanema parovale sp. nov.

(*Neometanema* gen. nov.), a marine phagotrophic euglenid with skidding motility. Protist 165, 452–472.

Leedale, G., 1967. Euglenoid Flagellates. Englewood Clffffs, N.J, Prentice-Hall.

Leedale, G., 2002. Class Euglenoidea Bütschli, 1884. In: Lee, J.J., Leedale, G., Bradbury, P. (Eds.), The Illustrated Guide to the Protozoa. Society of Protozoologists, Lawrence, Kansas, pp. 1136–1157, dated 2000.

Lemmermann, E., 1913. Flagellatae 2. Gustav Fischer. Jena.

Linton, E.W., Triemer, R.E., 1999. Reconstruction of the feeding apparatus in *Ploeotia costata* (Euglenophyta) and its relationship to other euglenoid feeding apparatuses. J. Phycol. 35, 313–324.

Lukeš, J., Leander, B.S., Keeling, P.J., 2009. Cascades of convergent evolution: the corresponding evolutionary histories of euglenozoans and dinoflagellates. Proc. Natl. Acad. Sci. U. S. A. 106 (Suppl. 1), 9963–9970.

Marande, W., Lukeš, J., Burger, G., 2005. Unique mitochondrial genome structure in diplonemids, the sister group of kinetoplastids. Eukaryot. Cell 4, 1137–1146.

Melkonian, M., Robenek, H., Rassat, J., 1982. Flagellar membrane specializations and their relationship to mastigonemes and microtubules in *Euglena gracilis*. J. Cell Sci. 55, 115–135.

Mignot, J.-P., 1961. Contribution à l'étude cytologique de *Scytomonas pusilla* (Stein) (Flagellé euglénien). Bull. Biol. Fr. Belg. 95, 665–678.

Mignot, J.P., 1962. Étude du noyau de l'Euglénien *Scytomonas pusilla* Stein, flagellé euglénien. Comptes Rend. Hebdo. Séanc. Acad. Sci. 254, 1864–1866.

Mignot, J.-P., 1963. Quelques particularités de l'ultrastructure d' *Entosiphon sulcatum* (Duj.) Stein, flagellé euglénien. Comptes Rend. Acad. Sci. 257, 2530–2533.

Mignot, J.-P., 1966. Structure et ultrastructure de quelques euglénomonadines. Protistologica 2, 51–117.

Mignot, J.-P., 1967. Affinités des euglénamonadines et des chloromonadines: remarques sur la sytématique des Euglénida. Protistologica 3, 25–60.

Montegut-Felkner, A.E., Triemer, R.E., 1994. Phylogeny of *Diplonema ambulator* (Larsen and Patterson): 1. Homologies of the flagellar apparatus. Eur. J. Protistol. 30, 227–237.

Norris, R.E., 1964. Studies on phytoplankton in Wellington Harbour. N. Z. J. Bot. 2, 258–278.

Page, F.C., 1988. A New Key to Freshwater and soil Gymnamoebae with Instructions for Culture. Freshwater Biological Association, Ambleside, Cumbria.

Patterson, D.J., Larsen, J., 1992. A perspective on protistan nomenclature. J. Protozool. 39, 125–131.

Patterson, D.J., Simpson, A.G.B., 1996. Heterotrophic flagellates from coastal marine and hypersaline sediments in Western Australia. Eur. J. Protistol. 32, 423–448.

Patterson, D.J., Zölffel, M., 1991. Heterotrophic flagellates of uncertain taxonomic position. In: Patterson, D.J., Larsen, J. (Eds.), The Biology of Free-Living Heterotrophic Flagellates. Clarendon Press, Oxford, pp. 427–476.

Pochman, A., 1953. Struktur Wachstum und Teilung der Körperhülle bei der Eugleninen. Planta 42, 478–548.

Preisig, H., 1979. Zwei neue Vertreter der farblosen Euglenophyta. Schweiz. Z. Hydrol. 41, 155–160.

Ritter von Stein, F., 1878. Der Organismus der Infusionsthiere. III. Der Organismus der Flagellaten I. Engelmann, Leipzig.

Raymann, K., Brochier-Armanet, C., Gribaldo, S., 2015. The two-domain tree of life is linked to a new root for the Archaea. Proc. Natl. Acad. Sci. U. S. A. 112 (21), 6670–6675, http://dx.doi.org/10.1073/pnas.1420858112.

Roy, J., Faktorová, D., Lukeš, J., Burger, G., 2007. Unusual mitochondrial genome structures throughout the Euglenozoa. Protist 158, 385–396.

Sandon, H., 1927. The Composition and Distribution of the Protozoan Fauna of the Soil. Oliver & Boyd, Edinburgh.

Saville Kent, W., 1880–1882. A Manual of the Infusoria. Bogue, London.

Shawhan, F.M., Jahn, T.L., 1947. A survey of the genus *Petalomonas* Stein (Protozoa; Euglenida). Trans. Am. Microsc. Soc. 66, 182–189.

Simpson, A.G.B., 1997. The identity and composition of the Euglenozoa. Arch. Protistenk. 148, 318–328.

Simpson, A.G.B., Inagaki, Y., Roger, A.J., 2006. Comprehensive multigene phylogenies of excavate protists reveal the evolutionary positions of "primitive" eukaryotes. Mol. Biol. Evol. 23, 615–625.

Simpson, A.G.B., Roger, A.J., 2004. Protein phylogenies robustly resolve the deep-level relationships within Euglenozoa. Mol. Phylogenet. Evol. 30, 201–212.

Skuja, H., 1934. Beitrag zur Algenflora Lettlands I. Acta Hort. Bot. Univ. Latt. 7, 25–85, dated 1932.

Solomon, J.A., Walne, P.L., Kivic, P.A., 1987. *Entosiphon sulcatum* (Euglenophyceae): flagellar roots of the basal body complex and reservoir region. J. Phycol. 23, 85–98.

Stechmann, A., Cavalier-Smith, T., 2003. Phylogenetic analysis of eukaryotes using heat-shock protein Hsp90. J. Mol. Evol. 57, 408–419.

Stokes, A.C., 1885. Some new infusoria from American fresh waters. Ann. Mag. Nat. Hist. series 5 (15), 437–449.

Stokes, A.C., 1888. A preliminary contribution toward a history of the freshwater Infusoria of the United States. J. Trenton. Nat. Hist. Soc. 1, 71–365.

Tong, S.M., 1997. Heterotrophic flagellates and other protists from Southampton Water, UK. Ophelia 47, 71–131.

Triemer, R.E., 1988. Ultrastructure of mitosis in *Entosiphon sulcatum* (Euglenida). J. Protozool. 35, 231–237.

Triemer, R.E., Farmer, M.A., 1991a. An ultrastructural comparison of the mitotic apparatus, feeding apparatus, flagellar apparatus and cytoskeleton in euglenoids and kinetoplastids. Protoplasma 164, 91–104.

Triemer, R.E., Farmer, M.A., 1991b. The ultrastructural organization of heterotrophic euglenids and its evolutionary implications. In: Patterson, D.J., Larsen, J. (Eds.), The Biology of Free-Living Heterotrophic Flagellates. Clarendon Press, Oxford, pp. 185–204.

Triemer, R.E., Fritz, L., 1987. Structure and operation of the feeding apparatus in a colorless euglenoid, *Entosiphon sulcatum*. J. Protozool. 34, 39–47.

von der Heyden, S., Chao, E.E., Vickerman, K., Cavalier-Smith, T., 2004. Ribosomal RNA phylogeny of bodonid and diplonemid flagellates and the evolution of Euglenozoa. J. Euk. Microbiol. 51, 402–416.

Withold, M., 2001. Untersuchung zur Ultrastruktur und Function des Schlundapparates (Siphons) von *Entosiphon sulcatum*. Ruhr-University Bochum, Bochum http://www-brs.ub.ruhr-uni-bochum.de/netahtml/HSS/Diss/MuetzeWitold/diss.pdf.

Woodhead, N., Tweed, R.D., 1960. Additions to the algal flora of Newfoundland. Part I: New and interesting algae in the Avalon Peninsula and central Newfoundland. Hydrobiologia 15, 309–362.

Yabuki, A., Chao, E.E., Ishida, K., Cavalier-Smith, T., 2012. *Microheliella maris* (Microhelida ord. n.), an ultrastructurally highly distinctive new axopodial protist species and genus, and the unity of phylum Heliozoa. Protist 163, 356–388.

Yamaguchi, A., Yubuki, N., Leander, B.S., 2012. Morphostasis in a novel eukaryote illuminates the evolutionary transition from phagotrophy to phototrophy: description of *Rapaza viridis* n. gen. et sp. (Euglenozoa, Euglenida). BMC Evol. Biol. 12, 29.

Yubuki, N., Edgcomb, V.P., Bernhard, J.M., Leander, B.S., 2009. Ultrastructure and molecular phylogeny of *Calkinsia aureus*: cellular identity of a novel clade of deep-sea euglenozoans with epibiotic bacteria. BMC Microbiol. 9, 16.

Yubuki, N., Simpson, A.G., Leander, B.S., 2013. Reconstruction of the feeding apparatus in *Postgaardi mariagerensis* provides evidence for character evolution within the Symbiontida (Euglenozoa). Eur. J. Protistol. 49, 32–39.

Zougman, A., Ziolkowski, P., Mann, M., Wisniewski, J.R., 2008. Evidence for insertional RNA editing in humans. Curr. Biol. 18, 1760–1765.